X-822

OAK RIDGE NATIONAL LABORATORY
Operated by
UNION CARBIDE NUCLEAR COMPANY
Division of Union Carbide Corporation
Post Office Box X
Oak Ridge, Tennessee

DATE: June 19, 1961

SUBJECT: Heat Transfer Analysis of Pebble Bed Reactors and Comparison with Prismatic Cores

TO: Listed Distribution

FROM: N. Ozisik
R. B. Korsmeyer
G. L. Rhoden

Abstract

The general analytical equations relating the core power density and the gas film temperature drop at the fuel surface to the principal reactor parameters are presented for both axial flow and radial flow pebble bed cores. Charts are included which show the power density and gas film temperature drop as functions of fuel ball diameter, pumping power-to-heat removal ratio, gas temperature rise per unit length of gas passage, and the gas pressure. The effects of voidage, system temperature and gas properties are considered along with factors causing hot spots. The effect on interior temperature of variations in the gas film heat transfer coefficient around the fuel surface was investigated with the IBM 704 computer for cases of interest.

Neglecting hot spots, the power density obtainable in the prismatic core is more than four times that of the pebble bed core for equal maximum fuel temperatures. The extra degree of freedom available in design of prismatic core coolant passages permits the designer always to select a combination of parameters that is superior to the optimum combination for the pebble bed reactor.

It is therefore clear that the fuel handling system, including perhaps the reactor maintenance, will have to be considerably more economical in the case of the pebble bed reactor in order for that reactor to compete with its prismatic counterpart.

Nomenclature

A = total core face area perpendicular to the direction of coolant flow, ft^2

a = outside radius of core, ft

C_p = specific heat, Btu/lb °F

D_s = ball diameter, ft

E = modulus of elasticity, psi

$F_{h,\Delta t}$ = hot spot factor for the gas film temperature drop due to variation of heat transfer coefficient around the ball

$F_{j,\Delta t}$ = hot spot factor for the gas film temperature drop at radial position J, dimensionless

$F_{j,\delta t}$ = hot spot factor for the gas temperature rise at radial position J, dimensionless

$F_{w,\Delta t}$ = hot spot factor for the gas film temperature drop at the wake of a cluster, dimensionless

f = friction factor, dimensionless

G_s = mass flow rate per unit core area perpendicular to the direction of flow, $lb/hr\text{-}ft^2$

G_o = mass flow rate per unit core area at the inlet of the radial flow cores, $lb/hr\text{-}ft^2$

g = mass-force conversion coefficient, 4.18×10^8, ft/hr^2

h = heat transfer coefficient, $Btu/hr\text{-}ft^2\text{-}°F$

K = core power density, $Btu/hr\text{-}ft^3$

K^* = core power density, kw/L

k = thermal conductivity, $Btu/hr\text{-}ft^2\text{-}°F/ft$

L = core length, ft

De = equivalent diameter (prismatic cores), ft.

M = molecular weight, lb/mol

n = ratio of outer radius to inner radius for the radial flow cores, dimensionless

P = pressure, lb/ft^2

ΔP = pressure drop, lb/ft^2

Pr = Prandtl number, dimensionless

Q = heat removal from the core, Btu/hr

q = heat removal, Btu/hr

r = core radius, ft

r_o = core radius at the inlet of the radial flow cores, ft

Re = Reynolds number, dimensionless

S = heat transfer area per unit core volume, ft^2/ft^3

t = temperature, °F

t_i = inlet temperature, °F

t_s = ball surface temperature, °F

t_c = ball center temperature, °F

δt = gas temperature rise, °F

$(\delta t/L)$ = gas temperature rise per unit core length, °F/ft

Δt = gas film temperature drop, °F

Δt_c = temperature difference between ball center and ball surface, °F

T = temperature, °R

V = core volume, ft^3

W = pumping power, Btu/hr

(W/Q) = pumping power-to-heat removal ratio, dimensionless

x = distance from gas inlet, ft

y = distance from ball center, ft

α = coefficient of thermal expansion, in/ in - °F

ϵ = void fraction, dimensionless

γ = ratio of the local core power density to the average core power density

λ = ratio to the length of pebble bed core to the length of prismatic core

μ = viscosity, lb/hr-ft

ρ = density, lb/ft^3

τ = ratio of the pressure of pebble bed core to the pressure of prismatic core

ν = Poisson's ratio, dimensionless

σ_t = tangential thermal stress, psi

ξ = ratio of the pumping power-to-heat removal ratio of the pebble bed core to the pumping power-to-heat removal ratio of prismatic core

Subscripts

e = equivalent

i = any radial section

j = a particular radial section

m = average

p = prismatic

Subscripts (cont.)

r	=	radial position at distance r from the core center
s	=	pebble bed
x	=	distance along the core from the gas inlet

INTRODUCTION AND SUMMARY

In the fall of 1960 two studies of the pebble bed reactor concept were completed at ORNL.[4][8] The first study involved the preliminary design of a 10 Mwt experimental reactor, and the second study was concerned with the design of an 800 Mwt power station. Extensive calculations of the heat transfer characteristics and temperature structures of these two reactors were carried out, but only part of the work was reported at the time. The purpose of this report is, therefore, to present the complete heat transfer analysis along with a more quantitative comparison of the pebble reactor with the streamlined, or "prismatic", type of reactor.

The general analytical equations relating the core power density and the gas film temperature drop at the fuel surface to the principal reactor parameters, both for the axial flow and the radial flow pebble-bed cores, were used to prepare charts showing the relations between the major parameters. In particular the core power density and gas film temperature drop are shown as functions of ball diameter, pumping power-to-heat removal ratio, gas temperature rise per unit length of gas passage, and the gas pressure in the operating ranges of interest. The effects of voidage, system temperature, and the properties of the gas used are also considered, along with the factors causing hot spots.

The possibility of hot spot formation in packed clusters of balls, especially in the vicinity of points of contact, was investigated. The effect of variations in the gas film heat transfer coefficient around the

balls on internal temperatures was investigated with the IBM 704 computer for the cases of interest. Charts are presented to show the temperature distribution in the core and the effects of radial variations in core voidage on temperature distribution.

Although the radial-flow pebble bed core has a characteristically low pressure drop, the radial mismatch of gas flow and power density and the neutron leakage at the center inlet make this concept very unattractive compared to the much simpler axial flow cores. Of the latter, the down-flow core is not subject to bed levitation, but the core support structure lies directly in the hot exit gas stream. Until the design of a reliable, dimensionally stable structure is demonstrated, however, only the axial upflow core may be seriously considered.

The high heat transfer coefficients obtainable in axial flow pebble-bed cores are accompanied by high pumping power requirements resulting from the eddy losses associated with expansion and contraction of the coolant passages in the direction of flow. Compared to the pebble-bed core, the heat transfer coefficient for a given mass flow rate is low in the prismatic core, but a higher flow rate can be obtained for the same pumping power-to-heat removal ratio. Neglecting hot spots, the power density obtainable in the prismatic core is more than four times that of the pebble-bed core for equal maximum fuel temperatures, and it is even greater when allowance is made for the wider variations in hot spots characteristic of a randomly packed bed.

The most realistic comparison is obtained between the two types of reactors, however, when each has been independently optimized to match

a given power output at fixed steam conditions. When this is done the prismatic reactor appears to be more attractive because the extra degree of freedom in the design of the coolant passages permits the designer always to select a combination of parameters that is superior to the optimum combination for the pebble bed reactor.

It is therefore clear that the fuel handling system, including perhaps reactor maintenance, will have to be considerably more economical in the case of the pebble bed reactor in order for that reactor to compete with its prismatic counterpart.

The General Analytical Equations

Using an energy balance coupled with the heat transfer coefficient and the friction pressure drop equations, the average core power density for an axial flow pebble bed reactor can be expressed as a function of the principal reactor parameters as follows: (derivation in Appendix A)

$$K_m = 192 \frac{\epsilon^{1.73}}{(1-\epsilon)^{0.735}} \frac{C_p^{1.577}}{\mu^{0.156}} \left(\frac{PM}{T}\right)^{1.154} D_s^{0.735} \left(\frac{\delta t_m}{L}\right)^{1.577} \left(\frac{W}{Q}\right)^{0.577} \quad (1)$$

The gas film temperature drop over the fuel element surface is not included in this equation; it is left as a variable quantity the magnitude of which depends upon the parameters on the right-hand side of Eq. (1), but it can be expressed as a function of these parameters, as shown in Eq. (2): (derivation in Appendix A)

$$\Delta t_m = 1.60 \frac{\epsilon^{0.52}}{(1-\epsilon)^{1.52}} \frac{C_p^{0.173}\, Pr^{0.66}}{\mu^{0.346}} \left(\frac{PM}{T}\right)^{0.346} D_s^{1.52} \left(\frac{\delta t_m}{L}\right)^{1.173} \left(\frac{W}{Q}\right)^{0.173} \quad (2)$$

For pebble bed reactors with cylindrical cores, it is possible to arrange the flow of coolant gas in the radial direction. In such cases, the foregoing equations, which are for the axial flow pebble-bed cores, cannot be used because, with the radial flow cores, the flow passage area varies in the radial direction. Using a similar procedure to that for the axial flow cores, the following equations were derived for the outward radial flow cores: (derivation in Appendix B)

The average core power density is:

$$K_m = 320 \frac{\epsilon^{1.73}}{(1-\epsilon)^{0.735}} \frac{C_p^{1.577}}{\mu^{0.156}} \left(\frac{PM}{T}\right)^{1.154} D_s^{0.735} \left(\frac{\delta t_m}{r_o}\right)^{1.577} \left(\frac{W}{Q}\right)^{0.577} \frac{1}{(n^2-1)(1-n^{-0.73})^{0.577}} \quad (3)$$

The gas film temperature drop at a distance r from the center of the core is:

$$\Delta t_{mr} = 3.06 \frac{\epsilon^{0.52}}{(1-\epsilon)^{1.52}} \frac{C_p^{0.173}\, Pr^{0.66}}{\mu^{0.346}} \left(\frac{PM}{T}\right)^{0.346} D_s^{1.52} \left(\frac{\delta t_m}{r_o}\right)^{1.173} \left(\frac{W}{Q}\right)^{0.173} \left(\frac{r}{r_o}\right)^{0.7} \frac{1}{(n^2-1)(1-n^{-0.73})^{0.173}}$$

It is to be noted that the film temperature drop at the outlet can be obtained by taking $r = a$.

Parametric Study of Pebble Bed Reactor Cores

The principal reactor parameters which affect the core design are all explicitly included in the foregoing equations. Once the type of coolant gas and the pressure level of the reactor are selected, it is convenient to plot K_m and Δt_m against the ball diameter. $(\delta t_m/L)$ and (W/Q) may be selected as the independent parameters in such a chart for the axial flow cores, while (n) and (W/Q) may be selected as independent parameters for the radial flow cores.

Figure 1 shows such a chart for the axial flow pebble-bed cores for $\epsilon = 0.39$ and helium as the coolant gas at a mean temperature of 950°F. In order to illustrate the effect of pressure in the operating ranges of interest, the charts were prepared for 1000, 600, and 300 pisa pressures. The data presented in Fig. 1 can easily be applied to other mean gas temperatures, voidages, and gases by multiplying the values of K_m and Δt_m obtained from this chart by the appropriate correction factors given in Fig. 2.

Fig. 1 can be used to design the core in the following manner. The reactor power, the gas pressure, and the gas temperature rise (δt_m) through the core should be chosen along with values for (K_m) and ($\delta t_m/L$). These fix the core diameter and the core length. The core diameter should be such that the corresponding pressure vessel thickness will not exceed the limit imposed by manufacturing feasibility, and the ratio of the core length to core diameter will satisfy the reactor physics requirements from the neutron economy standpoint. Having established suitable values for K_m and ($\delta t_m/L$), the chart in Fig. 1 can be used to determine values for (D_s) and (W/Q). The ball diameter should be such that the allowable thermal stress limits will not be exceeded. Knowing the properties of the fuel element material, the limiting thermal stress line can be evaluated and plotted on the chart. A typical limiting thermal stress line for the graphite balls is shown superimposed with dashed lines on Fig. 1, assuming the limiting stress is 2000 psi, the thermal conductivity is 8 Btu/hr-ft^2-°F/ft, the modulus of elasticity is 1.5×10^6 psi, Poisson's ratio is 0.3, and the

coefficient of thermal expansion is $3 \times 10^{-6}{}^{o}F$ (Appendix C). The pumping power-to-heat removal ratio for a good balance between capital charges and power costs is usually from 0.5 to 1.0%. However, in the case of axial flow pebble-bed unrestrained cores with upward coolant flow, levitation of the balls limits the pumping power-to-heat removal ratio to a value less than that economically justifiable. With the above limitations in mind, suitable values of (D_s) and (W/Q) can be determined from Fig. 1, and these define the corresponding value for Δt_m.

In a typical arrangement for radial flow pebble-bed reactors, the cooling gas enters the core through a cylindrical passage at the center and flows radially outward through the core. The core power density and the gas film temperature drop over the surface of the balls for such cores are given by Eqs. (3) and (4). The additional parameters introduced into these equations are r_o and n, where n is the ratio of the outer radius to inner radius of the core. Using Eqs. (3) and (4), parametric charts similar to those in Fig. 1 can be constructed for the radial flow cores if any two of the three parameters $(r_o, n, \delta t_m)$ are also fixed. Figure 3 shows such charts for the radial flow cores for which r_o and t_m were fixed, but n was taken as an independent parameter. From Eq. (4) it can be seen that the film temperature drop increases with the radius, and higher film temperature drops are expected to occur at the outer perimeter. Therefore, the film temperature drops given in Fig. 3 are for those at the outer perimeter of the core. The data in Fig. 3 can be adjusted for other gas mean temperatures, voidages and gases using the correction factors given in Fig. 2.

The data presented in Fig. 3 can be used in the design of outward radial flow pebble bed reactors by following a procedure similar to that given above for axial flow cores.

Fuel Element Temperature and Hot Spot Problems

The fuel element surface temperature is equal to the sum of the local gas temperature and the film temperature drop from the fuel element surface to the gas. The internal ball temperature drop may be added to the fuel element surface temperature to give the ball center temperature.

Neglecting the variation of power density in the core and the hot spots, the fuel surface and the fuel center temperatures at a distance x from the core inlet of the axial flow cores are:

$$t_{s,x} = t_{inlet} + \frac{x}{L} \delta t_m + \Delta t_m \qquad (5)$$

$$t_{c,x} = t_{s,x} + \Delta t_c$$

Variations in the core power density both in the axial and radial directions, coupled with nonuniformities in the coolant flow through the core cause some spots to run much hotter than others so that the above simple relations for the fuel element temperature need modification.

Recent Canadian research[1] indicates that the local heat transfer coefficient varies around the balls in a closely-packed infinite bed of spheres. For the coolant flow rates in the range of interest, the local heat transfer coefficients near points of contact of the balls were found

to be half or less of the average heat transfer coefficient for the ball as a whole. Such low local heat transfer coefficients tend to increase the local surface temperatures. In order to estimate this effect, the temperature distribution in the ball was calculated for several cases of interest using a generalized heat conduction code for the IBM-704 computer.[2] The relaxation nets used to divide the ball into differential sections and the manner in which the ball properties were computed in the differential sections are explained in Appendix D. The following simplifying assumptions were made:

1) Each ball has seven contact points uniformly distributed over the ball surface.

2) The heat transfer coefficient is a minimum at the contact point, increases with distance from this point, and has symmetry about this point.

Computations were made for 1-1/2-in.-diam graphite balls having a thermal conductivity of 10 Btu/hr-ft^2-°F/ft. The heat generation rate within the ball was assumed to be uniform and was taken as 50 w/cm^3.

Figures 4a, b, and c show the temperature distribution in such balls having an average film heat transfer coefficient of 610 Btu/hr-ft^2-°F for three different distributions of the heat transfer coefficient around the ball. Figures 4a and b are for average-to-minimum film heat transfer coefficient ratios of 2 and 3 respectively; while Fig. 4c is for a uniform heat transfer coefficient of 610 Btu/hr-ft^2-°F. The temperatures shown on the figures are all in degrees Fahrenheit above the reference bulk coolant temperature which was taken as zero. Figures 5a, b, and c are the results

of similar calculations for an average film coefficient of 305 Btu/hr-ft^2-°F.

From the results of these calculations it is concluded that varying the film coefficient over the ball surface while keeping its average value constant has little effect on the ball center temperature; only the temperatures near the surface are affected. For balls with a variable heat transfer coefficient, the film temperature drop at the hot spot may be from 20 to 40% higher than the temperature drop with a uniform heat transfer coefficient. The hot spot factor due to the variation of heat transfer coefficient around the ball will be represented below by $F_{h,\Delta t}$.

The variation in the voidage of pebble-bed cores is another factor which affects the coolant flow rate and consequently the fuel element temperature. In a randomly-packed bed of spheres the voidage at the wall is greater than the voidage at the center of the bed[3], and for small cylindrical cores this variation is quite pronounced. In order to estimate the effects on the gas temperature rise and the film drop of these variations in core voidage caused by the wall, an analysis was made for a simplified core model. It is assumed that the voidage varied only in the radial direction with symmetry about the central axis, and that there was no radial mixing of the coolant. The derivation of the hot spot factors for such a model is given in Appendix E, and the results (for axial flow cores) are as follows:

The hot spot factor for the gas temperature rise at a radial section j is:

$$F_{j,\delta t} = \frac{\sum_{i=1} A_i \frac{\epsilon_i^{1.73}}{(1-\epsilon_i)^{0.735}}}{A \frac{\epsilon_j^{1.73}}{(1-\epsilon_j)^{0.735}}} \tag{7}$$

and the hot spot factor for the film temperature drop over the ball surface at a radial section j is:

$$F_{j,\Delta t} = \left(F_{j,\delta t}\right)^{0.7} \left(\frac{1-\epsilon_e}{1-\epsilon_j}\right)^{1.3} \tag{8}$$

These factors can be evaluated only if the radial distribution of the core voidage is known.

Schwartz[3] gives the distribution of core voidage as a function of ball diameter and distance from the wall for cylindrical cores. These data indicate that voidage varies from about 60% at the wall to 30% in the core center for cores with core diameter to ball diameter ratios in the range of 8 to 16.

In a randomly-packed bed of spheres, closely-packed clusters may be formed in some regions. The coolant flow is reduced through such clusters because of the increased resistance to flow. The reduced flow rate increases the gas temperature rise. The coolant velocity in the wake of the cluster is also reduced, causing a reduction in the local heat transfer coefficient and an increase in the film temperature drop. The hot spot factor which applies to the film temperature drop in the wake of the cluster will be represented by the symbol, $F_{w,\Delta t}$. The maximum surface and internal

fuel temperatures at any given point in an axial flow core can be obtained by introducing these hot spot factors into equations (5) and (6) in the following manner:

$$(t_s)_{j,x} \approx t_{in} + \Delta t_m \left(F_{h,\Delta t}\, F_{j,\Delta t}\, F_{w,\Delta t}\, \gamma_{j,x}\right) + \frac{\delta t_m}{L} F_{j,\delta t} \int_c^x \gamma_j \, dx \qquad (5\text{-a})$$

$$(t_c)_{j,x} \approx t_{in} + \Delta t_m \left(F_{j,\Delta t}\, F_{w,\Delta t}\, \gamma_{j,x}\right) + \frac{\delta t_m}{L} F_{j,\delta t} \int_o^x \gamma_j \, dx + \Delta t_c\, \gamma_{j,x} \qquad (6\text{-a})$$

where

$$\Delta t_c = \frac{K_m}{6k\,(1-\epsilon)} \left(\frac{D_\varepsilon}{2}\right)^2 \quad \text{(see Appendix C)}$$

The core power density distribution for a 10-Mwt, axial flow, 18-in.-dia, 10-ft-long, cylindrical, pebble-bed core with 1.5-in.-dia balls is shown in Fig. 6.[4] In this core the gas inlet temperature was 550°F, the average gas temperature rise 700°F, and the average film temperature drop 130°F. A simplified estimate of the hot spot temperatures for this reactor is given in Table I, assuming a uniform voidage throughout the core. However, the voidage is not uniform at the core wall and the non-uniformity cannot be neglected where the ratio of core-to-ball diameter is small. By assuming that the voidage varied in a manner similar to that given by Schwartz[3], the hot spot factors, $F_{i,\delta t}$ and $F_{i,\Delta t}$ were calculated from equations (7) and (8), and are given in Table II as a function of distance from the core wall.

TABLE I

Simplified Hot Spot Temperature Estimate
for the 10 Mwt Pebble-Bed Reactor Experiment
(Uniform Core Voidage)

Gas inlet temperature	550°F
Average gas temperature rise	700°F
Average film temperature drop	130°F
Average temperature drop through ball	170°F
Hot zone factors for film temperature drop:	
Power density Factor, $\gamma_{j,x}$	1.5
Wake Factor, $F_{w,\Delta t}$	1.5
Non-uniform heat transfer coeff. Factor, $F_{h,\Delta t}$	1.3
Hot zone factor for the gas temperature rise:	1.6
Film temperature drop at the hot spot, (130 x 1.5 x 1.5 x 1.3)	= 380°F
Gas temperature at the hot spot, (550 + 1.6 x 700)	= 1670°F
Hot ball surface temperature	= 2050°F
Ball temperature drop in the hot zone, (1.5 x 170)	= 255°F
Hot ball internal temperature	= 2305°F

These factors, together with the other hot spot factors, were used in estimating the ball center, ball surface and gas temperatures at the top and bottom regions of the core for the power distribution shown in Fig. 6. The resulting temperature distribution in the core is shown in Fig. 7 for the case of no radial gas mixing. The temperature distribution of a uniform voidage core was also included on this figure for comparison. For the case of uniform voidage, temperatures are higher at the wall, which is consistent

with the power distribution of Fig. 6. But, for the variable voidage, the increased gas flow near the wall depresses the gas temperature in that region, shifting the maximum gas temperature away from the wall. An isothermal plot of gas temperature for the core with variable voidage is shown in Fig. 8. Since no radial mixing of the coolant was considered in the calculations, the results are pessimistic. However, the results indicate the nature of the problem, the approximate magnitude of the effects, and the location of the hot zones.

The temperature distribution for a 20-ft diameter axial flow pebble-bed core[8] was calculated from the power distribution given by a multigroup calculation and is shown in Fig. 9. Because the voidage variation caused by the wall extends to about three ball diameters from the wall and affects a small region compared with the core diameter, a uniform core voidage was assumed for the calculations. However, higher voidage near the wall will cause some reduction in the gas temperature in the wall region from that shown in Fig. 9 without any pronounced effect on the temperature in other regions.

TABLE II

Factors for Film Temperature Drop and Gas Temperature Rise Resulting from Variable Core Voidage for the 10 Mwt Pebble Bed Reactor Experiment (4)

Distance in Ball Diameters From the Wall	$F_{i,\Delta t}$ Film Temperature Drop Factor	$F_{i,\delta t}$ Gas Temperature Rise Factor
0 - 0.25	1.1	0.3
0.25 - 0.50	1.1	0.8
0.50 - 1.00	1.2	1.3
1 - 2	1.3	1.7
2 - 6 (Core-center)	1.4	2.2

A Comparison of Pebble-Bed Cores with Cores Having Prismatic Fuel Elements

The high transfer coefficients obtainable in pebble-bed cores, or in cores with variable coolant flow cross sections, are usually accompanied by high pumping power requirements. This results from the eddy losses associated with expansion and contraction of the coolant passage in the direction of flow. In cores having prismatic fuel elements (i.e., tubes, plates, etc.) the coolant flow passages are uniform longitudinally. Compared with the pebble bed core, the heat transfer coefficient for a given mass flow rate is low in the prismatic core; but a high flow rate can be obtained for a given pumping power-to-heat removal ratio in the prismatic core.

It is important, therefore, to compare the characteristic reactor sizes and operating pressures associated with these two types of core, for the same output, recognizing, of course, that the optimum design conditions are not the same. In other words, the most meaningful comparison is one in which the two reactors have been independently optimized to deliver a given

net power at fixed steam conditions. This comparison is best arrived at by development of the power density and gas film temperature drop ratios of the two cases in terms of the various parameters already used.

The average core power density for prismatic cores is (App. F):

$$K_m = 2670\,\epsilon \left[\frac{C_p^{1.556}}{\mu^{0.111}}\right]\left[\frac{PM}{T}\right]^{1.111} D_e^{0.666}\left[\frac{\delta t_m}{L}\right]^{1.556}\left[\frac{W}{Q}\right]^{0.556} \qquad (9)$$

and the film temperature drop is:

$$\Delta t_m = 52.7\left[\frac{C_p^{1.111}\,\mu^{0.778}}{k\,Pr^{0.4}}\right]\left[\frac{PM}{T}\right]^{0.222} D_e^{1.333}\left[\frac{\delta t_m}{L}\right]^{1.111}\left[\frac{W}{Q}\right]^{0.111} \qquad (10)$$

A completely general correlation, arrived at by ratioing the equations for the densities and gas film temperature drops for the two cases is too cumbersome to use. It is better, therefore, to employ equations (1), (2), (9), and (10) in relation to a specific reactor concept. For example, a fairly large power station for which reactors of these types might be attractive would be one designed to produce, say, 325 Mwe (800 Mwt) a steam temperature of 1050°F.[8] The coolant gas and its inlet and outlet temperatures would be the same in each case. With helium as the coolant, and effective inlet and outlet temperatures of 550°F and 1250°F, respectively, equations (1), (2), (9), and (10) give:

$$K_{mp} = 1.99 \times 10^5\,\epsilon_p\,P_p^{1.111}\,D_e^{0.666}\left[\frac{1}{L_p}\right]^{1.556}\left[\frac{W}{Q}\right]_p^{0.556} \qquad (11)$$

$$\Delta t_{mp} = 3.04 \times 10^4\,P_p^{0.222}\,D_e^{1.333}\left[\frac{1}{L_p}\right]^{1.111}\left[\frac{W}{Q}\right]_p^{0.111} \qquad (12)$$

$$K_{ms} = 1.40 \times 10^{4} \frac{\epsilon_s^{1.73}}{(1 - \epsilon_s)^{0.735}} P_s^{1.154} D_s^{0.735} \left[\frac{1}{L_s}\right]^{1.577} \left[\frac{W}{Q}\right]_s^{0.577} \quad (13)$$

$$\Delta t_{ms} = 882 \left[\frac{\epsilon_s^{0.52}}{(1 - \epsilon_s)^{1.52}}\right] P_s^{0.346} D_s^{1.52} \left[\frac{1}{L_s}\right]^{1.173} \left[\frac{W}{Q}\right]_s^{0.173} \quad (14)$$

where subscripts p and s refer to the prismatic and the pebble bed cores respectively. The core lengths appear independently because the reactor powers have not yet been taken into account.

Rather than deal in terms of power density, the power station designer is more directly interested in the size of the reactor which he must enclose in a pressure vessel. The right circular cylinder of largest volume which can be enclosed in a sphere of given diameter has an aspect ratio (L/D_c) of 0.7. However, a reflected core of this geometry which has the highest neutron efficiency has an aspect ratio of 0.92, although there is not much loss in economy for aspect ratios between 0.7 and 0.92. Since very large pressure vessels of spherical form are cheaper than cylindrical vessels with domed ends, the shape of the pressure vessel does not enter into the comparison. The choice of aspect ratio does not, therefore, affect the comparison importantly, and equal values for the prismatic and pebble-bed cores have been arbitrarily chosen although the choice biasses the comparison slightly in favor of the pebble bed concept.

Thus:

$$\frac{K_{mp}}{K_{ms}} = \frac{L_s^3}{L_p^3} \tag{15}$$

In order to simplify the comparison, the core length, pressures and pumping power-to-heat removal ratios of the two cases are expressed in the following way:

$$\begin{aligned} L_s &= \lambda L_p \\ P_s &= \tau P_p \\ (W/Q)_s &= \xi (W/Q)_p \end{aligned} \tag{16}$$

The relations between corresponding dimensions of the prismatic and pebble bed cores are obtained by combining equations (11), (13), (15), and (16) to yield:

$$\lambda = 6.43\left[\frac{\epsilon_p^{0.702}(1-\epsilon_s)^{0.516}}{\epsilon_s^{1.216}}\right]\left[\frac{1}{\tau^{0.811}\,\xi^{0.405}}\right]\left[\frac{D_e^{0.468}}{D_s^{0.516}}\right]\left[\frac{L_p^{0.015}}{P_p^{0.032}\left(\frac{W}{Q}\right)_p^{0.015}}\right] \tag{17}$$

Similarly, equations (12), (14), and (16) yield:

$$\frac{\Delta t_{mp}}{\Delta t_{ms}} = 34.5\left[\frac{(1-\epsilon_s)^{1.52}}{\epsilon_s^{0.52}}\right]\left[\frac{\lambda^{1.173}}{\tau^{0.346}\,\xi^{0.173}}\right]\left[\frac{D_e^{1.333}}{D_s^{1.52}}\right]\left[\frac{L_p^{0.062}}{P_p^{0.124}\left(\frac{W}{Q}\right)_p^{0.062}}\right] \tag{18}$$

or, eliminating λ,

$$\frac{\Delta t_{mp}}{\Delta t_{ms}} = 307 \left[\frac{\epsilon_p^{0.824}(1 - \epsilon_s)^{2.125}}{\epsilon_s^{1.947}} \right] \left[\frac{1}{\tau^{1.298}\, \xi^{0.649}} \right] \left[\frac{D_e^{1.882}}{D_s^{2.125}} \right] \left[\frac{L_p^{0.079}}{P_p^{0.161} \left(\frac{W}{Q}\right)_p^{0.079}} \right] \quad (19)$$

In equations (17) and (19) the exponents of the terms in the last brackets are so small that the average values for these terms may be used without significant error over the operating ranges of interest. In the ranges of L_p = 5ft to 15ft, pressures from 300 to 700 psia, and (W/Q) = 0.003 to 0.015, the values of the brackets in equations (17) and (19) may be taken as 0.774 and 0.298 respectively with an extreme error of only ± 3.2% in equation 17 and ± 19% in equation 19. Hence equations (17) and (19) become approximately

$$\lambda = 4.98 \left[\frac{\epsilon_p^{0.702}(1 - \epsilon_s)^{0.516}}{\epsilon_s^{1.216}} \right] \left[\frac{1}{\tau^{0.811}\, \xi^{0.405}} \right] \left[\frac{D_e^{0.468}}{D_s^{0.516}} \right] \quad (20)$$

$$\frac{\Delta t_{mp}}{\Delta t_{ms}} = 91.5 \left[\frac{\epsilon_p^{0.824}(1 - \epsilon_s)^{2.125}}{\epsilon_s^{1.947}} \right] \left[\frac{1}{\tau^{1.298}\, \xi^{0.649}} \right] \left[\frac{D_e^{1.882}}{D_s^{2.125}} \right] \quad (21)$$

Thus the core sizes are directly related to four characteristic groups: the voidages, the gas pressures, the equivalent diameters of the flow passages, and the pumping power-to-heat removal ratios. The gas film temperature drops are similarly related.

The voidage in pebble-bed cores is not a variable if the fuel is of uniform size, and its value is approximately 0.39[3][9] for reasonably large bed (compared to fuel diameter). Substituting $\epsilon_s = 0.39$ in equations (20) and (21), yield:

$$\lambda = 12.1\left[\frac{\epsilon_p^{0.702}}{\tau^{0.811}\,\xi^{0.405}}\right]\left[\frac{D_e^{0.468}}{D_s^{0.516}}\right] \tag{22}$$

$$\frac{\Delta t_{mp}}{\Delta t_{ms}} = 199\left[\frac{\epsilon_p^{0.824}}{\tau^{1.298}\,\xi^{0.649}}\right]\left[\frac{D_e^{1.882}}{D_s^{2.125}}\right] \tag{23}$$

Consideration of Voidage in the Prismatic Core

It is clear from equation (22) that the prismatic core will be considerably smaller than the pebble bed core for equal operating pressures. Under this condition there is an incentive to hold the prismatic core voidage to a low value in order to minimize fuel cycle costs[8], and a void fraction close to 0.14 would be chosen. On the other hand, if the designer should prefer a lower gas pressure for the prismatic core (i.e. a larger core) the void fraction need not be held as low. A fraction as high as 0.25 might be acceptable although not necessarily optimum. Substantially higher fractions would not be given much consideration because of the increasing penalty associated with fuel cycle costs or reactor size without a corresponding reduction in other problems or costs. Let us choose a value of 0.20 as representative of well-designed, high-performance prismatic cores. Equations (22) and (23) become:

$$\lambda = 3.91\left[\frac{D_e^{0.468}}{D_s^{0.516}}\right]\left[\frac{1}{\tau^{0.811}\,\xi^{0.405}}\right] \tag{24}$$

$$\frac{\Delta t_{mp}}{\Delta t_{ms}} = 53.7 \left[\frac{D_e^{1.882}}{D_s^{2.125}}\right] \left[\frac{1}{\tau^{1.298}\ \xi^{0.649}}\right] \qquad (25)$$

Fig. 10 shows a comparison of the core length, core volume and film temperature drop for the prismatic and pebble bed cores as obtained from equations (24) and (25), in terms of the equivalent hydraulic diameters and fuel ball sizes. The curves shown are for the particular combinations of pressure ratios and pumping power-to-heat removal ratios shown. The comparison shows immediately that the prismatic core is considerably smaller for the same power output than its pebble bed counterpart, or its operating pressure and pumping power are lower. On the other hand, the gas film temperature drop is generally higher in the prismatic core if the core is much smaller than the pebble bed core. Considering the fact that prismatic fuel elements are easily designed to have much lower internal temperature drops than the matching pebble bed fuel elements, higher surface temperatures can be tolerated without exceeding the maximum allowable fuel temperature. Furthermore, the core radial temperature distribution can be made quite uniform by orificing the fuel channel inlets in the prismatic core, a step impractical for the pebble bed core, thus enhancing the tolerance for high average fuel surface temperatures.

Axial Flow Pebble Bed Limitations

Since the fuel levitation problem is aggravated as the fuel ball size is reduced, the designer is limited in the power densities he can achieve in unrestrained axial upflow beds. As a result, either uneconomically low power densities and pumping power-to-heat removal ratios are accepted, or schemes of unproven feasibility are resorted to in order to prevent

the fuel from fluidizing or bouncing in the gas stream. In the pebble bed reactor chosen here for comparison[8] the design was optimized with respect to all these parameters, and even then it required fuel balls 2.5 inches in diameter and was limited to an average power density of 6.6 w/cm^3. The W/Q had to be held to 0.003 whereas a value of 0.01 is acceptable for the prismatic cores. In this particular reactor the core height was 12.4 ft, the average gas film temperature drop was 126°F and the gas pressure was 700 psia.

In conclusion, the fuel handling, and perhaps the reactor maintenance, for the pebble bed reactor will have to be considerably easier and more economical than that for the prismatic reactors for the pebble bed reactor to be competitive.

REFERENCES

1. J. Wadsworth, "Experimental Examination of Local Processes in Packed Beds of Homogeneous Spheres", NRC-5895, Feb 1960. National Research Council of Canada.

2. T. B. Fowler and E. R. Volk, "Generalized Heat Conduction Code for the IBM-704 Computer", ORNL-2734.

3. Sanderson & Porter, "Design and Feasibility Study of a Pebble Bed Reactor-Steam Power Plant, NYOO-8753, Vol. I, Fig 2.1-2.

4. A. P. Fraas, et al, "Preliminary Design of a 10-Mw(t) Pebble-Bed Reactor Experiment", ORNL CF-60-10-63 (revised), May 8, 1961.

5. S. Timoshenko and J. N. Goodier, "Theory of Elasticity", McGraw-Hill Co.

6. McAdams, "Heat Transmission", 2nd edition, McGraw-Hill Book Co., p. 119.

7. Glasstone, "Principals of Nuclear Engineering".

8. A. P. Fraas, et al, "Design Study of a Pebble-Bed Reactor Power Plant", ORNL CF-60-12-5 (revised), May 11, 1961.

9. Progress Report, Pebble Bed Reactor Program, June 1958 to May 1959, NYO-2373.

APPENDIX A

Heat Transfer and Pressure Drop Relations for Axial Flow Pebble Beds

An expression for the core power density as a function of the principal system parameters can be derived as follows.

The friction factor for a randomly-packed bed of spheres is:[4]

$$f = 7.5 \frac{(1-\epsilon)^{1.27}}{\epsilon^3} Re^{-0.27} \tag{A-1}$$

where

$$Re = \frac{G_s D_s}{\mu} \tag{A-2}$$

The heat removal from the core is:

$$Q = G_s A C_p \delta t_m \tag{A-3}$$

The average core power density may be defined as:

$$K_m = \frac{Q}{V} = \frac{Q}{A L} \tag{A-4}$$

The relationships for pressure drop and pumping power are:

$$\Delta P = 2f \frac{G_o^2}{\rho g} \frac{L}{D_s}$$

$$= \frac{15 (1-\epsilon)^{1.27}}{\epsilon^3} \frac{\mu^{0.27}}{\rho D_s^{1.27}} G_s^{1.37} L \tag{A-5}$$

and

$$W = A \frac{\Delta P G_s}{778 \rho} \tag{A-6}$$

From Eqs. (A-3) and (A-6):

$$\frac{W}{Q} = \frac{1}{778} \frac{\Delta P}{\rho C_p \delta t_m} \tag{A-7}$$

Combining Eqs. (A-5) and (A-7) gives:

$$\frac{W}{Q} = \frac{15}{778} \frac{(1-\epsilon)^{1.27}}{\epsilon^3} \frac{G_s^{1.73}\ \mu^{0.27}}{\rho^2 g\ C_p\ D_s^{1.27}} \left(\frac{\delta t_m}{L}\right)^{-1} \tag{A-8}$$

From Eqs. (A-3) and (A-4):

$$G_s = \frac{K_m L}{C_p\ \delta t_m} \tag{A-9}$$

Substituting (A-9) into (A-8) and solving for K_m:

$$K_m = \left(\frac{778\ g}{15}\right)^{0.577} \left(\frac{W}{Q}\right)^{0.577} \frac{\epsilon^{1.73}}{(1-\epsilon)^{0.735}} \frac{C_p^{1.577}\ \rho^{1.154}\ D_s^{0.735}}{\mu^{0.156}} \left(\frac{\delta t_m}{L}\right)^{1.577} \tag{A-10}$$

Assuming the coolant to be a perfect gas:

$$\rho = \frac{PM}{1544\ T} \tag{A-11}$$

Substituting Eq. (A-11) into Eq. (A-10):

$$K_m = 192 \frac{\epsilon^{1.73}}{(1-\epsilon)^{0.735}} \frac{C_p^{1.577}}{\mu^{0.156}} \left(\frac{PM}{T}\right)^{1.154} D_s^{0.735} \left(\frac{\delta t_m}{L}\right)^{1.577} \left(\frac{W}{Q}\right)^{0.577} \tag{A-12}$$

One important parameter not included in Eq. (A-12) is the film temperature drop. It can be derived by considering the heat transferred from the surface of the fuel balls as follows.

The heat transfer surface per unit core volume is:

$$S = \frac{6(1-\epsilon)}{D_s}\ ft^2/\ ft^3 \tag{A-13}$$

Hence,

$$K_m = h\left[\frac{6\,(1-\epsilon)}{D_s}\right]\Delta t_m \qquad \text{(A-14)}$$

From Ref. 4:

$$h = 0.5\,(1-\epsilon)^{0.3}\,G_s\,C_p\,Pr^{-0.66}\,Re^{-0.3} \qquad \text{(A-15)}$$

Subtituting Eq. (A-9) into Eq. (A-15) and eliminating G:

$$h = 0.5\,(1-\epsilon)^{0.3}\,C_p^{0.3}\,Pr^{-0.66}\,\frac{\mu^{0.3}}{D_s^{0.3}}\,K_m^{0.7}\left(\frac{\delta t_m}{L}\right)^{-0.7} \qquad \text{(A-16)}$$

Substituting Eq. (A-16) into Eq. (A-14):

$$\Delta t_m = \frac{1}{3}\,\frac{D_s^{1.3}}{(1-\epsilon)^{1.3}}\,\frac{Pr^{0.66}}{C_p^{0.3}\,\mu^{0.3}}\,K_m^{0.3}\left(\frac{\delta t_m}{L}\right)^{0.7} \qquad \text{(A-17)}$$

Substituting Eq. (A-12) into Eq. (A-17):

$$\Delta t_m = 1.60\,\frac{\epsilon^{0.52}}{(1-\epsilon)^{1.52}}\,\frac{C_p^{0.173}\,Pr^{0.66}}{\mu^{0.346}}\left(\frac{PM}{T}\right)^{0.346} D_s^{1.52} \qquad \text{(A-18)}$$

$$\left(\frac{\delta t_m}{L}\right)^{1.173}\left(\frac{W}{Q}\right)^{0.173}$$

Equation (A-12) gives the core power density in a core of uniform voidage and uniform power distribution. Either Eq. (A-17) or Eq. (A-18) can be used to obtain the film temperature drop at the fuel ball surface.

For the cores with power output varying throughout the core, the power density and film temperature drop at any point are:

$$K = \gamma\,K_m$$
$$\Delta t = \gamma\,\Delta t_m \qquad \text{(A-19)}$$

where

$$\gamma = \frac{\text{local core power density}}{\text{average core power density}}$$

APPENDIX B

Heat Transfer and Pressure Drop Relations for Radial Flow Pebble Beds

The core power density can be derived as a function of the parameters of a radial flow pebble bed as follows.

From Eq. (A-7):

$$\frac{W}{Q} = \frac{1}{778} \cdot \frac{\Delta P}{\rho C_p \, \delta t_m} \tag{B-1}$$

$$\Delta P = \int_{r_o}^{a} dP \tag{B-2}$$

From Eq. (A-5):

$$dP = C_1 \, G_s^{1.73} \, dr \tag{B-3}$$

where

$$C_1 = \frac{15}{g} \frac{(1 - \epsilon)^{1.27}}{\epsilon^3} \cdot \frac{\mu^{0.27}}{\rho D_s^{1.27}} \tag{B-4}$$

$$G_s = G_o \cdot \frac{r_o}{r} \tag{B-5}$$

Substituting Eq. (B-5) and Eq. (B-3) in Eq. (B-2) and integrating:

$$\Delta P = \frac{C_1 \, (G_o \, r_o)^{1.73}}{0.73} \left[r_o^{-0.73} - a^{-0.73} \right] \tag{B-6}$$

Define n:

$$n = \frac{a}{r_o} \tag{B-7}$$

Substituting Eq. (B-6) and Eq. (B-7) into Eq. (B-1) and solving for G_o:

$$G_o = \left(56\varepsilon\right)^{0.577} \rho^{0.577} C_p^{0.577} \left(\frac{\delta t_m}{r_o}\right)^{0.577} \frac{(W/Q)^{0.577}}{C_1^{0.577} \left[1 - n^{-0.73}\right]^{0.577}} \tag{B-8}$$

By definition the power density is:

$$K_m = \frac{Q}{\pi (a^2 - r_o^2) L} = \frac{2\pi r_o L G_o C_p \delta t_m}{\pi (a^2 - r_o^2) L}$$

Or
$$K_m = \frac{2 G_o C_p \delta t_m}{(n^2 - 1) r_o} \tag{B-9}$$

Substituting Eqs. (B-4), (B-8), and (A-11) into Eq. (B-9):

$$K_m = \frac{320 \dfrac{\epsilon^{1.73}}{(1 - \epsilon)^{0.735}} \dfrac{C_p^{1.577}}{\mu^{0.156}} \left(\dfrac{PM}{T}\right)^{1.154} D_s^{0.735} \left(\dfrac{\delta t_m}{r_o}\right)^{1.577} \left(\dfrac{W}{Q}\right)^{0.577}}{(n^2 - 1)(1 - n^{-0.73})^{0.577}} \tag{B-10}$$

The film temperature drop at the surface of the ball can be evaluated as follows:

From Eq. (A-14):

$$\Delta t_{mr} = \frac{K_m D_s}{6h (1 - \epsilon)} \tag{B-11}$$

From Eq. (A-15), Eq. (A-2) and Eq. (B-5):

$$L = 0.5 (1 - \epsilon)^{0.3} \left(\frac{G_o r_o}{r}\right)^{0.7} C_p Pr^{-0.66} \frac{\mu^{0.3}}{D_s^{0.3}} \tag{B-12}$$

Solving Eq. (B-9) for G_o and substituting in Eq. (B-12):

$$h = \frac{0.5}{(2)^{0.7}} \frac{(1-\epsilon)^{0.3}}{D_s^{0.3}} \frac{C_p^{0.3}\ \mu^{0.3}}{Pr^{0.66}} \left(\frac{\delta t_m}{r_o}\right)^{-0.7} K_m^{0.7} \left[r_o \frac{(n^2-1)}{r}\right]^{0.7} \tag{B-13}$$

Substituting Eq. (B-13) into Eq. (B-11):

$$\Delta t_{mr} = 0.542 \frac{1}{(1-\epsilon)^{1.3}} \frac{Pr^{0.66}}{C_p^{0.3}\ \mu^{0.3}} D_s^{1.3}\ K_m^{0.3} \left[\left(\frac{\delta t_m}{r_o}\right)^{0.7} \frac{r}{r_o (n^2-1)}\right]^{0.7} \tag{B-14}$$

Substituting Eq. (B-10) into Eq. (B-14) we obtain Δt_{mr} in terms of the pumping power-to-heat removal ratio:

$$\Delta t_{mr} = \frac{3.062 \frac{\epsilon^{0.52}}{(1-\epsilon)^{1.52}} \frac{C_p^{0.173}\ Pr^{0.66}}{\mu^{0.346}} \left(\frac{PM}{T}\right)^{0.346} D_s^{1.52}}{(n^2-1)\left(1-n^{-0.73}\right)^{0.173}} \cdots$$

$$\frac{\left(\frac{\delta t_m}{r_o}\right)^{1.173} \left(\frac{W}{Q}\right)^{0.173} \left(\frac{r}{r_o}\right)^{0.7}}{} \tag{B-15}$$

APPENDIX C

Thermal Stress and Temperature Drop Within the Ball

The tangential stress in a ball is:[5]

$$\sigma_t = \frac{\alpha E}{1-\nu}\left[\frac{2}{(D_s/2)^3}\int_o^{D_s/2} T\,y^2\,dy + \frac{1}{y^3}\int_o^{y} T\,y^2\,dy - T\right] \qquad (C\text{-}1)$$

where

y = distance from the ball center

Assuming uniform heat generation rate in the ball, the heat balance equation for heat transfer at distance y from the ball center is:

$$\frac{K}{1-\epsilon}\left(\frac{4}{3}\,\pi y^3\right) = -k\,(4\,\pi y^2)\,\frac{dT}{dy} \qquad (C\text{-}2)$$

Integrating Eq. (C-2) with the boundary condition $T = 0$ at $y = D_s/2$ gives:

$$T = \frac{K}{6K\,(1-\epsilon)}\left[\left(\frac{D_s}{2}\right)^2 - y^2\right] \qquad (C\text{-}3)$$

Substituting Eq. (C-3) into Eq. (C-1) and integrating between $y = 0$ and $y = D_s/2$ gives the tangential stress at the ball surface as follows:

$$\sigma_t = \frac{\alpha E}{15k\,(1-\nu)}\left(\frac{D_s}{2}\right)^2 \frac{K}{1-\epsilon} \qquad (C\text{-}4)$$

The temperature drop between the ball center and the ball surface can be found by substituting $y = 0$ in Eq. (C-3):

$$\Delta t_c = \frac{K}{6k\,(1-\epsilon)}\left(\frac{D_s}{2}\right)^2 \qquad (C\text{-}5)$$

APPENDIX D

Effects of Local Variations in Heat Transfer Coefficients on the Temperature Distribution and Thermal Stress Within a Fuel Ball

The three-dimensional steady-state heat conduction problem for the ball was reduced to a two dimensional problem and relaxation calculations were carried out assuming:

1) uniform heat generation rate within the ball,
2) uniform thermal conductivity,
3) uniform bulk gas temperature around the ball,
4) uniformly distributed contact points over the ball surface, and
5) a gas-film heat transfer coefficient distribution symmetrical about the contact point.

Figure 11 shows the model used to approximate the two-dimensional heat conduction problem in the ball. In this figure, point A corresponds to the ball center, B to a contact point, and AB is the axis of symmetry. Hence, this figure represents the portion of the sphere obtained by rotating this figure about the AB axis. It was assumed that no heat is conducted across AB and AC, and that the heat transfer coefficient increases along AC in the C direction. For seven points of contact the angle θ is about 45 degrees.

Consider a nodal point O at a distance $(m.\Delta \ell)$ from the AB axis. Assume that point O is thermally connected to the four adjacent points, each a distance $(\Delta \ell)$ apart from O, as shown in Fig. 11.

The temperature of the nodal point, T_o, must satisfy the equation:

$$\sum_{i=1}^{4} C_{i-o} (T_i - T_o) + Q_o = 0 \qquad \text{(D-1)}$$

where

C_{i-o} = the thermal conductance (i.e., kx area/length) between points i and o,

Q_o = the rate of heat generation at o.

Because of symmetry about the AB axis, C_{i-o} and Q_o can be evaluated as follows:

$$C_{1-o} = C_{3-o} = \frac{k\, 2\pi\, m\, \Delta\ell\, \Delta\ell}{\Delta\ell} = 2\pi\, k\, m\, \Delta\ell \qquad \text{(D-2)}$$

$$C_{2-o} = \frac{k\, 2\pi \left(m\, \Delta\ell - \frac{1}{2}\Delta\ell\right)\Delta\ell}{\Delta\ell} = 2\pi\, k \left(m - \frac{1}{2}\right)\Delta\ell \qquad \text{(D-3)}$$

$$C_{4-o} = \frac{k\, 2\pi \left(m\, \Delta\ell + \frac{1}{2}\Delta\ell\right)\Delta\ell}{\Delta\ell} = 2\pi\, k \left(m + \frac{1}{2}\right)\Delta\ell \qquad \text{(D-4)}$$

$$Q_o = 2\pi\ m\, \Delta\ell\, \Delta\ell\, q \qquad \text{(D-5)}$$

where

q = heat generation rate per unit volume of the ball

k = thermal conductivity of the ball material

m = 1, 2, 3, etc.

Dividing the entire surface into fine square nets and evaluating C_{i-o} and Q_o in a manner as described above, the problem was coded using the "Generalized Heat Conduction Code" for the IBM-704 computer.[2]

APPENDIX E

Hot Spot Factors Resulting from Variable Core Voidage

Consider an axial flow, cylindrical pebble-bed reactor core and assume that the core voidage varies only in the radial direction with cylindrical symmetry about the central axis. Divide the core into (n) concentric cylinders. Assume that each of these sections is at some constant voidage, and that the pressure drop across the length of each section is the same regardless of the voidage.

Consider any section i. The pressure drop for this section is (from Eq. (A-5)):

$$\Delta P = \frac{15}{g} \frac{(1 - \epsilon_i)^{1.27}}{\epsilon_i^3} \frac{\mu_i^{0.27}}{\rho_i} \frac{L}{D_s^{1.27}} G_i^{1.73} \qquad \text{(E-1)}$$

Since ΔP, L, and D_s are assumed to be the same for all sections, Eq. (E-1) can be solved for G_i as follows:

$$G_i = K \frac{\epsilon_i^{1.73}}{(1 - \epsilon_i)^{0.735}} \frac{\rho_i^{0.578}}{\mu_i^{0.156}} \qquad \text{(E-2)}$$

where

K = the term which is the same for all sections.

Now, define (G_e) as that gas flow rate (lb/hr-ft^2) which would result if the core voidage were uniform over the whole core cross section and equal to the mean voidage (ϵ_e) of the core. Then, for the same total

gas flow rate through the core, we have:

$$G_e A = \sum_{i=1}^{i=n} G_i A_i \qquad \text{(E-3)}$$

where

A = total cross section area of the core = $\sum_{i=1}^{n} A_i$

A_i = cross section area of section i

Now, consider a particular section j. Assume that the heat to be removed from the section j is the same when the voidage in this section is replaced by ϵ_e and the gas flow rate by G_e. Then:

$$q_j = A_j C_p G_j \delta t_{mj} = A_j C_p G_e \delta t_{me}$$

or

$$\delta t_{mj} = \frac{G_e}{G_j} \delta t_{me} \qquad \text{(E-4)}$$

Substituting value of G from Eq. (E-2) into Eq. (E-5) with appropriate subscripts:

$$\delta t_{mj} = \frac{\sum_{i=1}^{i=n} A_i \dfrac{\epsilon_i^{1.73}}{(1-\epsilon_i)^{0.735}} \dfrac{\rho_i^{0.578}}{\mu_i^{0.156}}}{A\left[\dfrac{\epsilon_j^{1.73}}{(1-\epsilon_j)^{0.735}} \dfrac{\rho_j^{0.578}}{\mu_j^{0.156}}\right]} \delta t_{me} \simeq F_{j,\delta t}\, \delta t_{me} \qquad \text{(E-6)}$$

Neglecting the effect of temperature on ρ and μ, the hot spot factor for the gas temperature rise in section j, $F_{j,\delta t}$, becomes:

$$F_{j,\delta t} = \frac{\sum_{i=1}^{n} A_i \dfrac{\epsilon_i^{1.73}}{(1-\epsilon_i)^{0.735}}}{A\left[\dfrac{\epsilon_j^{1.73}}{(1-\epsilon_j)^{0.735}}\right]} \qquad \text{(E-7)}$$

The hot spot factor for the film temperature drop for section j, $F_{j,\Delta t}$, can be evaluated by considering the heat transfer in this section as follows:

$$q_i = (vol)_j S_e h_e \Delta t_e = (vol)_j S_j h_j \Delta t_j \qquad \text{(E-8)}$$

From Eq. (A-15):

$$h = K' (1-\epsilon)^{0.3} G^{0.7} \mu^{0.3} \qquad \text{(E-9)}$$

where

K' = the term which is the same for all sections.

From Eq. (A-13):

$$S = \frac{6(1-\epsilon)}{D_s} \qquad \text{(E-10)}$$

Substituting Eqs. (E-9) and (E-10) into Eq. (E-8) with appropriate subscripts and solving for Δt_j:

$$\Delta t_j = \left(\frac{G_e}{G_j}\right)^{0.7} \left(\frac{1-\epsilon_e}{1-\epsilon_j}\right)^{1.3} \left(\frac{\mu_e}{\mu_j}\right)^{0.3} \Delta t_{me} \qquad \text{(E-11)}$$

From Eq. (E-4) and E-6):

$$\frac{G_e}{G_j} = F_{j,\delta t} \qquad \text{(E-12)}$$

Substituting Eq. (E-12) into Eq. (E-11):

$$\Delta t_j = \left(F_{j,\delta t} \right)^{0.7} \left(\frac{1 - \epsilon_e}{1 - \epsilon_j} \right)^{1.3} \left(\frac{\mu_e}{\mu_j} \right)^{0.3} \Delta t_{me} \simeq F_{j,\Delta t} \; \Delta t_{me} \qquad \text{(E-13)}$$

Neglecting the temperature effect on μ, the hot spot factor for the film temperature drop for section j becomes:

$$F_{j,\Delta t} = (F_{j,\delta t})^{0.7} \left(\frac{1 - \epsilon_e}{1 - \epsilon_j} \right)^{1.3} \qquad \text{(E-14)}$$

APPENDIX F

Heat Transfer and Pressure Drop Equations for Prismatic Fuel Elements

The term prismatic core refers to those cores having longitudinally uniform flow passages, such as given by tubular or rectangular fuel elements.

Following a procedure similar to that in Appendix A, the core power density for the prismatic cores can be calculated as follows:

$$f = 0.046 Re^{-0.2} \quad \text{Ref (6)} \tag{F-1}$$

$$Re = \frac{G D_e}{\mu} \tag{F-2}$$

In a core with uniform power distribution, the heat removal from the core is:

$$Q = (A\epsilon) G C_p \delta t_m \tag{F-3}$$

The average core power density may be defined as:

$$K_m = \frac{Q}{\text{core volume}} = \frac{Q}{A L} \tag{F-4}$$

The pressure drop and the pumping power are given by:

$$\Delta P = 2f \frac{G^2}{\rho g} \frac{L}{D_e}$$

$$= \frac{0.092}{g} \frac{G^{1.8} \mu^{0.2}}{\rho} \frac{L}{D_e^{1.2}} \tag{F-5}$$

and,

$$W = (A \epsilon) G \frac{\Delta P}{778 \rho} \tag{F-6}$$

From Eqs. (F-3) and (F-6):

$$\frac{W}{Q} = \frac{1}{778} \frac{\Delta P}{\rho C_p \delta t_m} \tag{F-7}$$

Combining Eqs. (F-5) and (F-7):

$$\left(\frac{W}{Q}\right) = \frac{0.092}{778\, g} \frac{G^{1.8}\, \mu^{0.2}}{\rho^2\, C_p\, D_e^{1.2}} \frac{L}{\delta t_m} \tag{F-8}$$

From Eqs. (F-3) and (F-4):

$$G = \frac{K_m}{\epsilon C_p} \frac{L}{\delta t_m} \tag{F-9}$$

Substituting Eq. (F-9) into Eq. (F-8) and solving for K_m:

$$K_m = \left(\frac{778\, g}{0.092}\right)^{0.556} \left(\frac{W}{Q}\right)^{0.556} \epsilon \left[\frac{C_p^{1.555}\, \rho^{1.111}\, D_e^{0.666}}{\mu^{0.111}}\right] \left(\frac{\delta t_m}{L}\right)^{1.555} \tag{F-10}$$

Assuming the coolant to be a perfect gas:

$$\rho = \frac{PM}{1544\, T} \tag{F-11}$$

Substituting Eq. (F-11) into Eq. (F-10):

$$K_m = (2.67 \times 10^3)\, \epsilon \frac{C_p^{1.555}}{\mu^{0.111}} \left(\frac{PM}{T}\right)^{1.111} D_e^{0.666} \left(\frac{\delta t_m}{L}\right)^{1.556} \left(\frac{W}{Q}\right)^{0.556} \tag{F-12}$$

The gas film temperature drop can be derived as follows:

$$S = \frac{4\epsilon}{D_e}\ ft^2/ft^3 \tag{F-13}$$

$$K_m = h\,S\,\Delta t_m = h\left(\frac{4\epsilon}{D_e}\right)\Delta t_m \qquad \text{(F-14)}$$

$$h = 0.023\,\frac{k}{D_e}\,Re^{0.8}\,Pr^{0.4} \qquad \text{Ref (7)}$$

$$= 0.023\,\frac{k\,Pr^{0.4}}{\mu^{0.8}}\,\frac{1}{D_e^{0.2}}\,G^{0.8} \qquad \text{(F-15)}$$

Substituting Eq. (F-9) into Eq. (F-15):

$$h = 0.023\left(\frac{1}{\epsilon^{0.8}}\right)\left(\frac{k\,Pr^{0.4}}{C_p^{0.8}\,\mu^{0.8}}\right)\left(\frac{L}{\delta t_m}\right)^{0.8}\frac{K_m^{0.8}}{D_e^{0.2}} \qquad \text{(F-16)}$$

Substituting Eq. (F-16) into Eq. (F-14) and solving for Δt_m:

$$\Delta t_m = \frac{1}{0.092}\left(\frac{1}{\epsilon^{0.2}}\right)\left(\frac{C_p^{0.8}\,\mu^{0.8}}{k\,Pr^{0.4}}\right)\left(\frac{\delta t_m}{L}\right)^{0.8} D_e^{1.2}\,K_m^{0.2} \qquad \text{(F-17)}$$

Substituting Eq. (F-12) into Eq. (F-17), to eliminate K_m, we get:

$$\Delta t_m = 52.7\left(\frac{C_p^{1.111}\,\mu^{0.778}}{k\,Pr^{0.4}}\right)\left(\frac{PM}{T}\right)^{0.222} D_e^{1.333}\left(\frac{\delta t_m}{L}\right)^{1.111}\left(\frac{W}{Q}\right)^{0.111} \qquad \text{(F-18)}$$

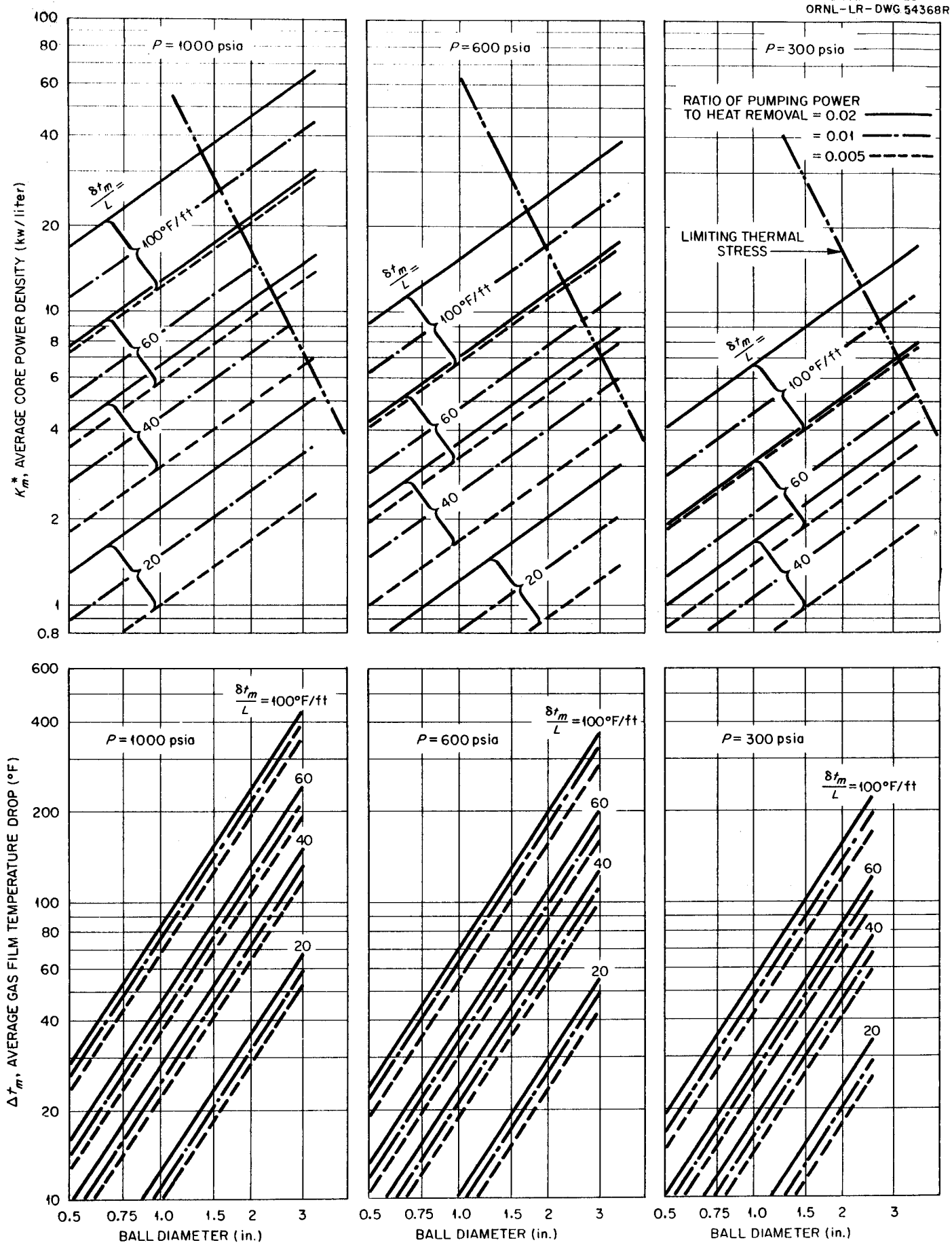

Fig. 1. Axial Flow Pebble Bed Reactor Core; Core Power Density and Gas Film Temperature Drop vs Ball Diameter.

UNCLASSIFIED
ORNL-LR-DWG 54369R

FACTORS FOR OTHER GASES:

K_m^* FOR CO_2 = 1.60 (K_m^* FROM FIG. 1) Δt_m FOR CO_2 = 1.66 (Δt_m FROM FIG. 1)

K_m^* FOR N_2 = 0.87 (K_m^* FROM FIG. 1) Δt_m FOR N_2 = 1.51 (Δt_m FROM FIG. 1)

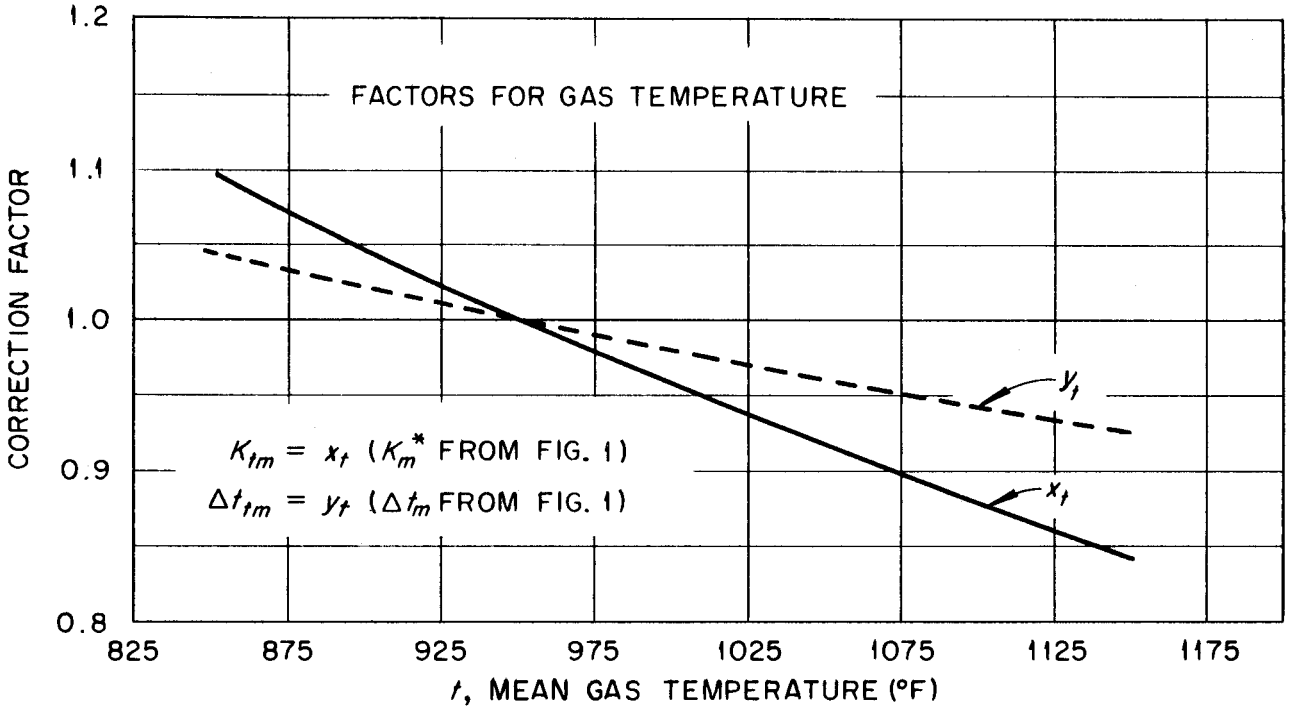

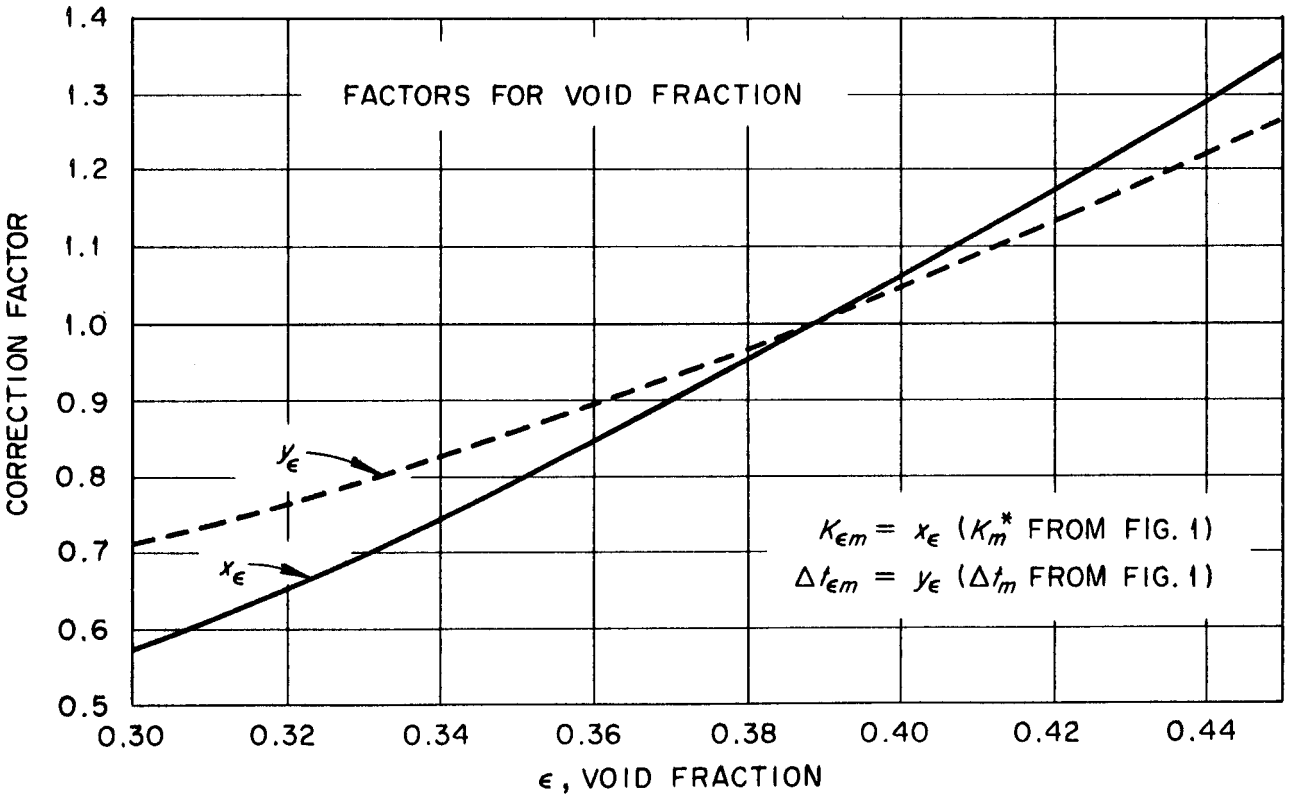

Fig. 2. Curves for Correcting Fig. 1 and 3 for Changes in System Temperature Level, Void Fraction, or Coolant Gas.

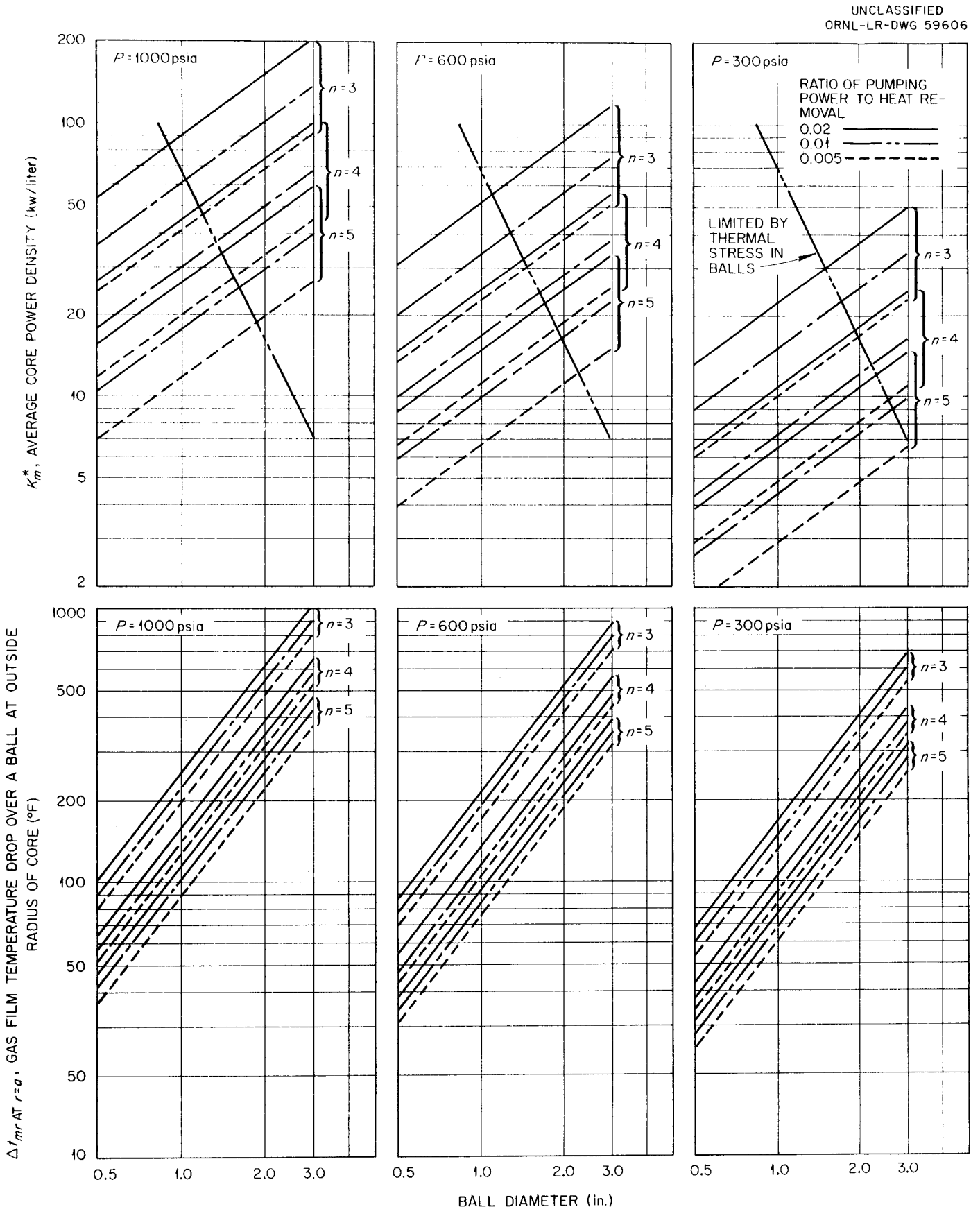

Fig. 3. Radial Flow Pebble Bed Reactor Core; Core Power Density and Gas Film Temperature Drop vs Ball Diameter. $\delta t_m = 800°F$, $r_0 = 2$ ft.

UNCLASSIFIED
ORNL-LR-DWG 54391R

NOTE: NUMBERS GIVE TEMPERATURE DROP, T (°F), FROM POINT IN BALL TO BULK FREE STREAM TEMPERATURE.

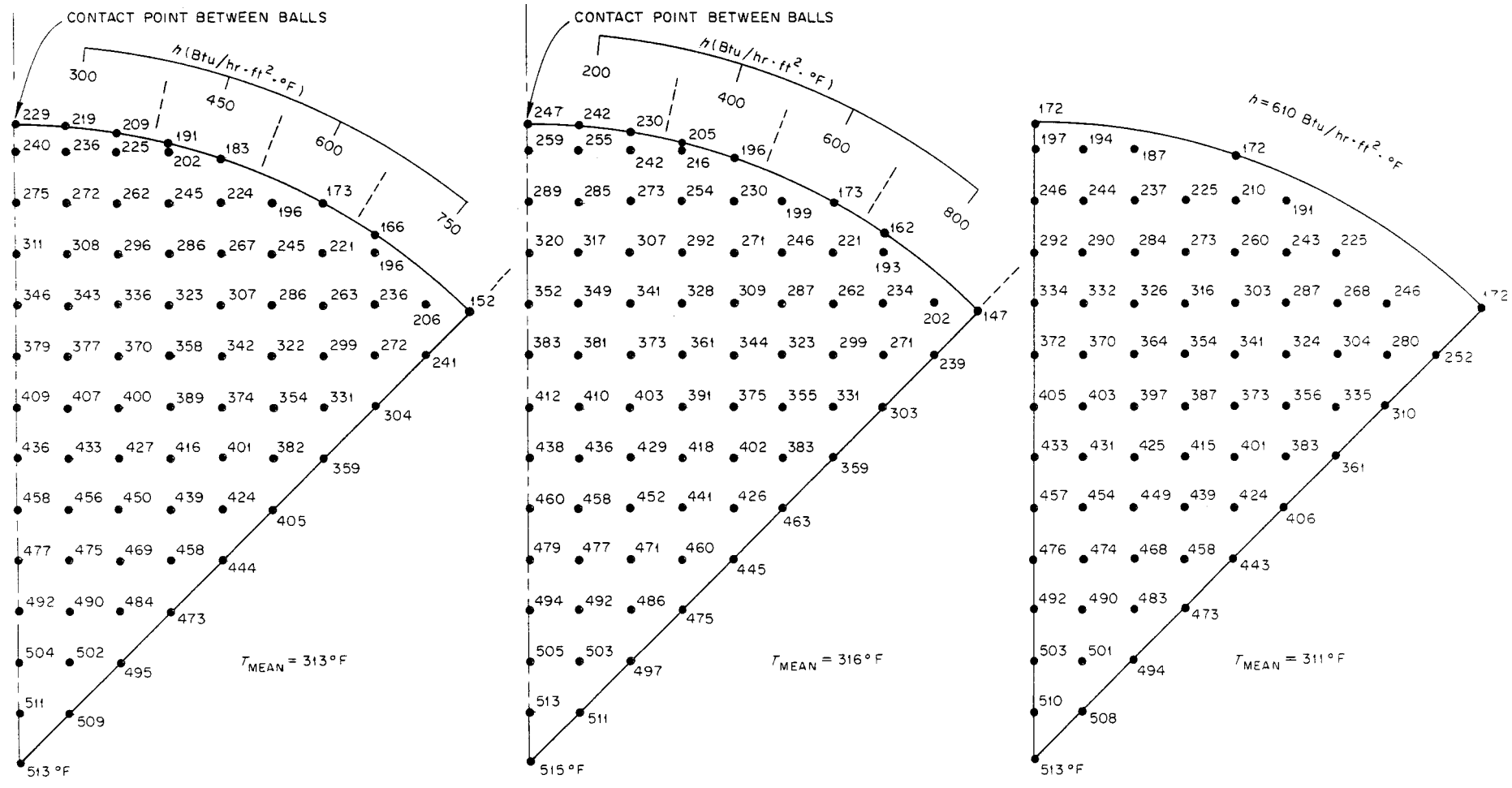

(a) LOCAL FILM COEFFICIENT

$\frac{h_{AV}}{h_{MIN}} \cong 2$

(b) LOCAL FILM COEFFICIENT

$\frac{h_{AV}}{h_{MIN}} \cong 3$

(c) UNIFORM FILM COEFFICIENT

Fig. 4. Temperature Distribution in Fuel Ball Based on an Average Film Coefficient, h, of 610 Btu/hr·ft^2·°F, a Heat Generation Rate of 50 kw/liter, a Ball Thermal Conductivity of 10 Btu/hr·ft·°F, and a Ball Diameter of 1.5 in.

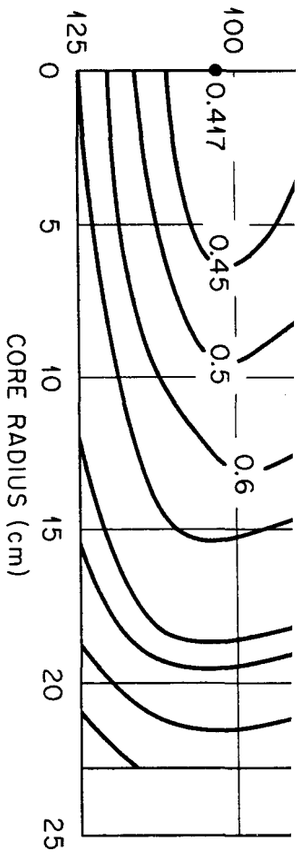

Fig. 6. Power Distribution of 10 Mw(t) Pebble Bed Reactor with Control Blades Withdrawn. (4)

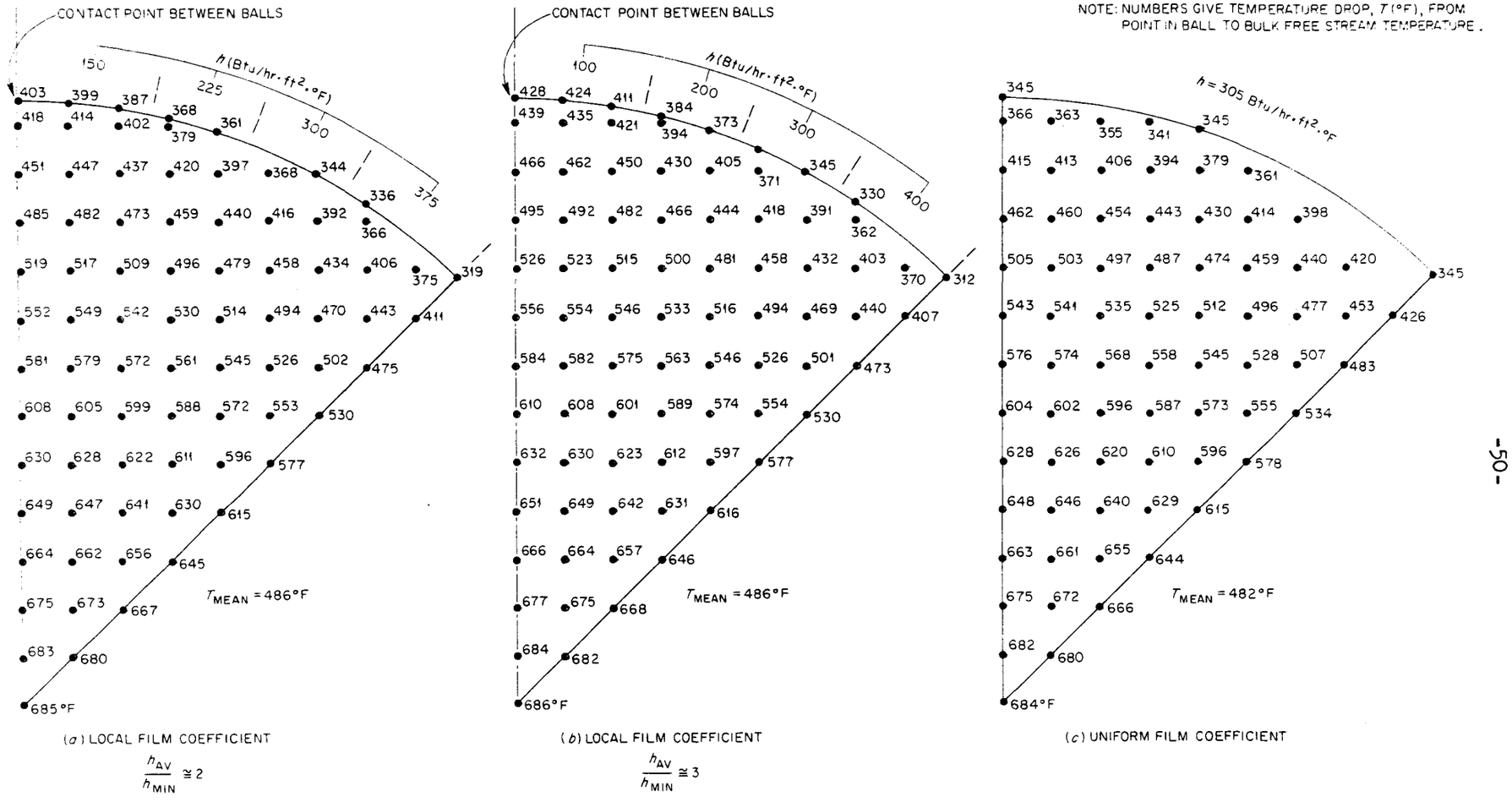

Fig. 5. Temperature Distribution in Fuel Ball Based on an Average Film Coefficient, h, of 305 Btu/hr·ft^2·°F, a Heat Generation Rate of 50 kw/liter, a Ball Thermal Conductivity of 10 Btu/hr·ft·°F, and a Ball Diameter of 1.5 in.

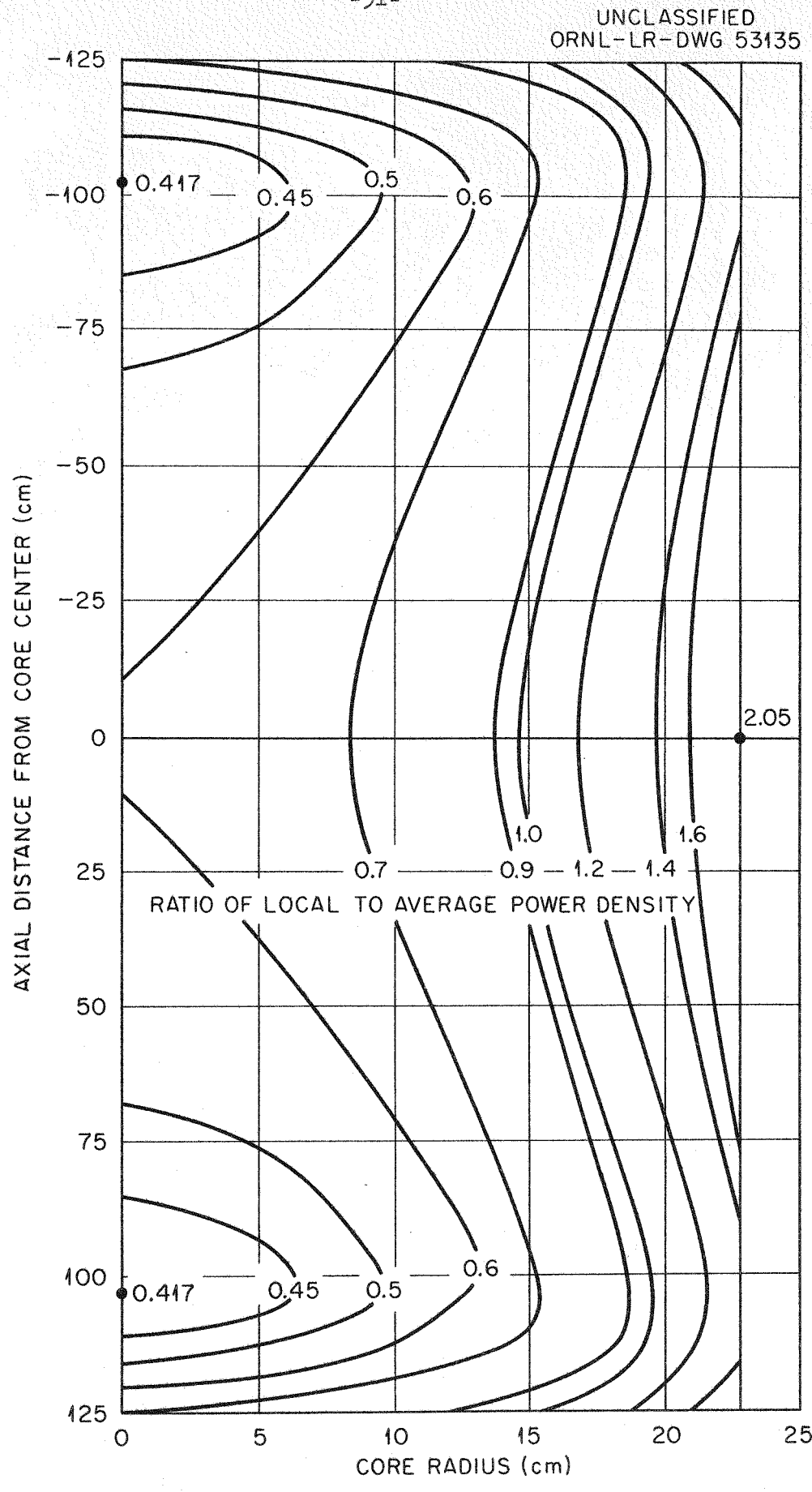

Fig. 6. Power Distribution of 10 Mw(t) Pebble Bed Reactor with Control Blades Withdrawn. (4)

UNCLASSIFIED
ORNL-LR-DWG 59607

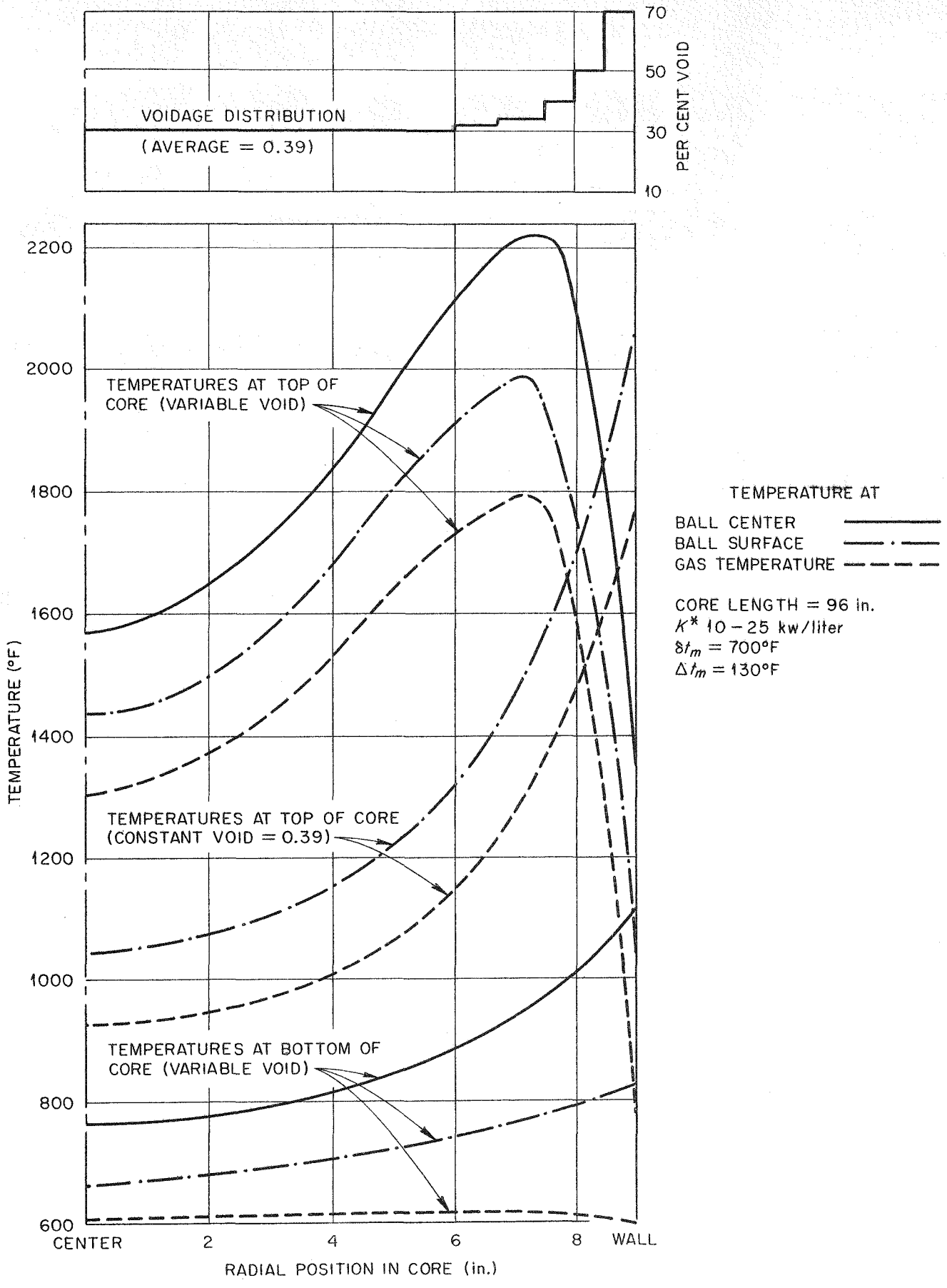

Fig. 7. Temperature and Voidage Distribution in PBRE.

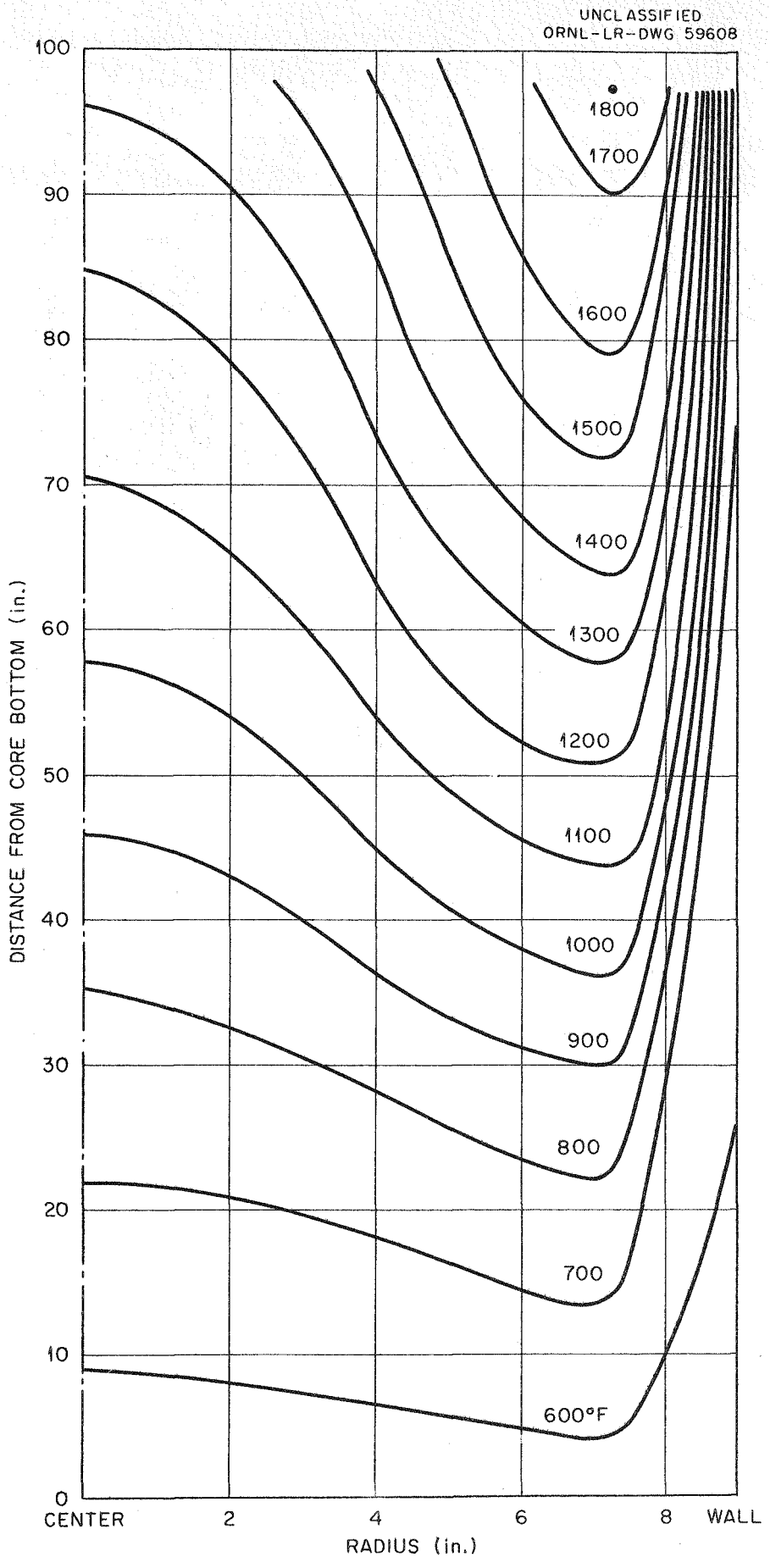

Fig. 8. Gas Temperature Distribution in PBRE.
(Assuming No Radial Gas Mixing)

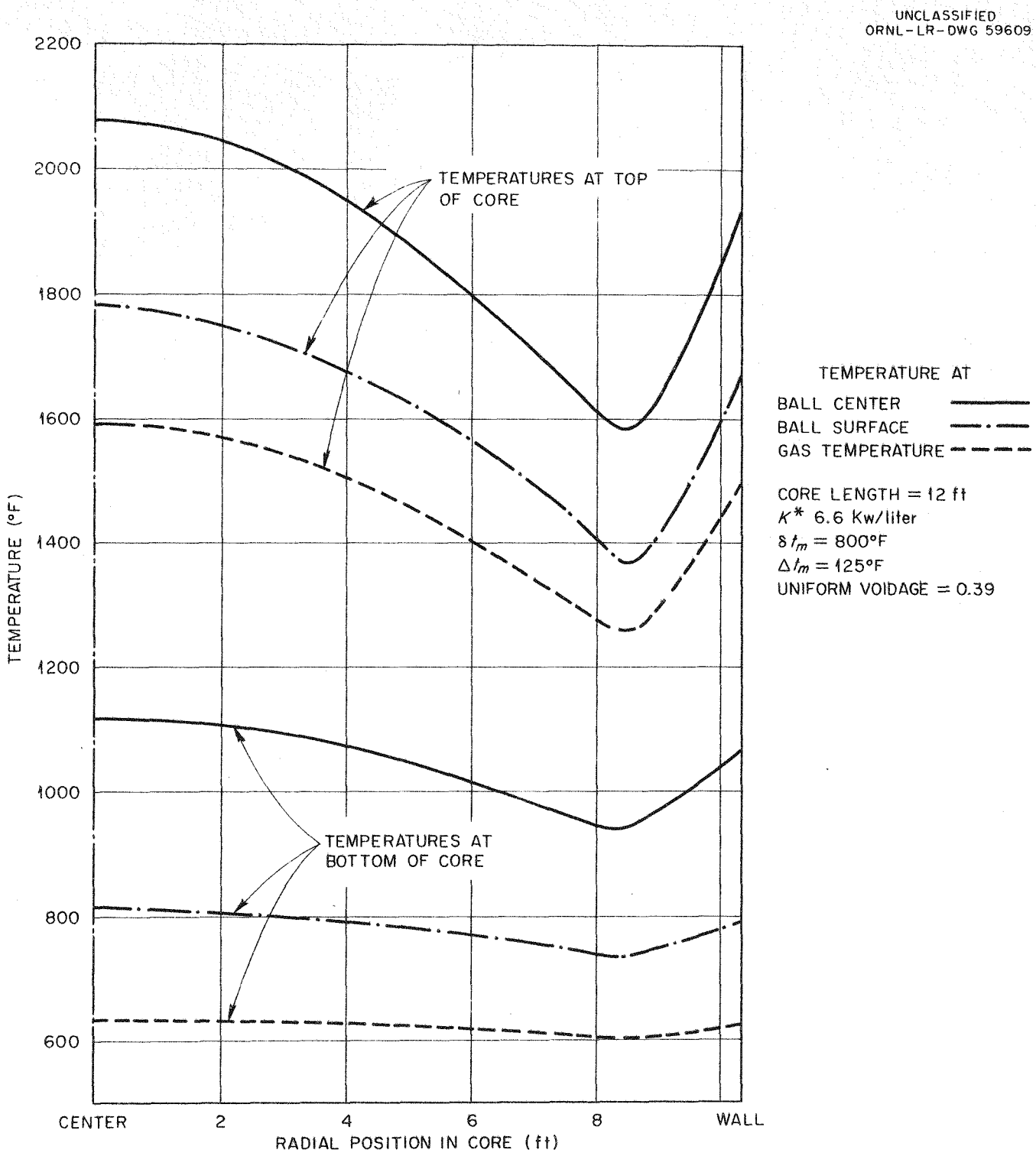

Fig. 9. Temperature Distribution in PBR.

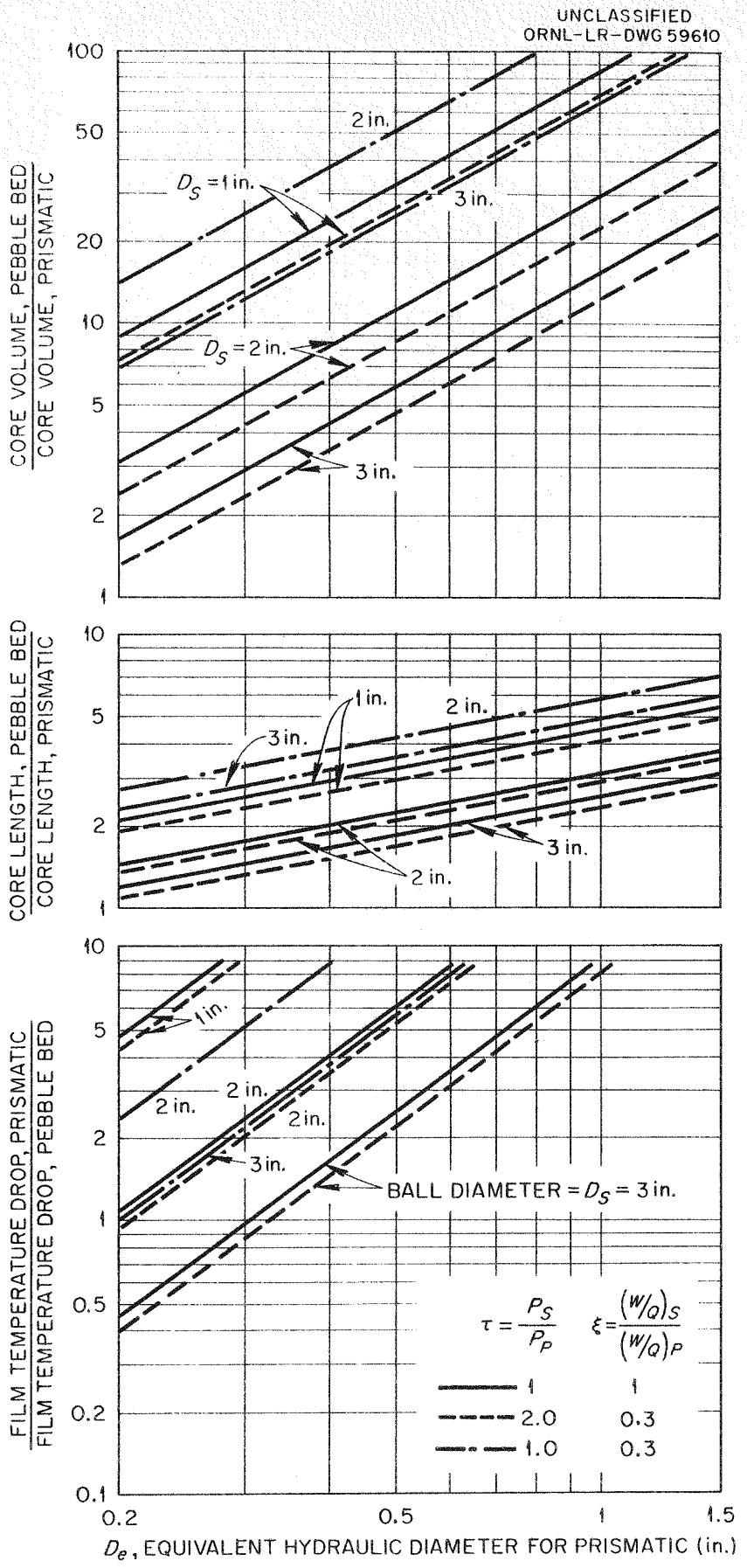

Fig. 10. Comparison of Axial-Flow Pebble Bed Cores with Cores Having Prismatic Fuel Elements. (Prismatic Core Voidage = 0.20)

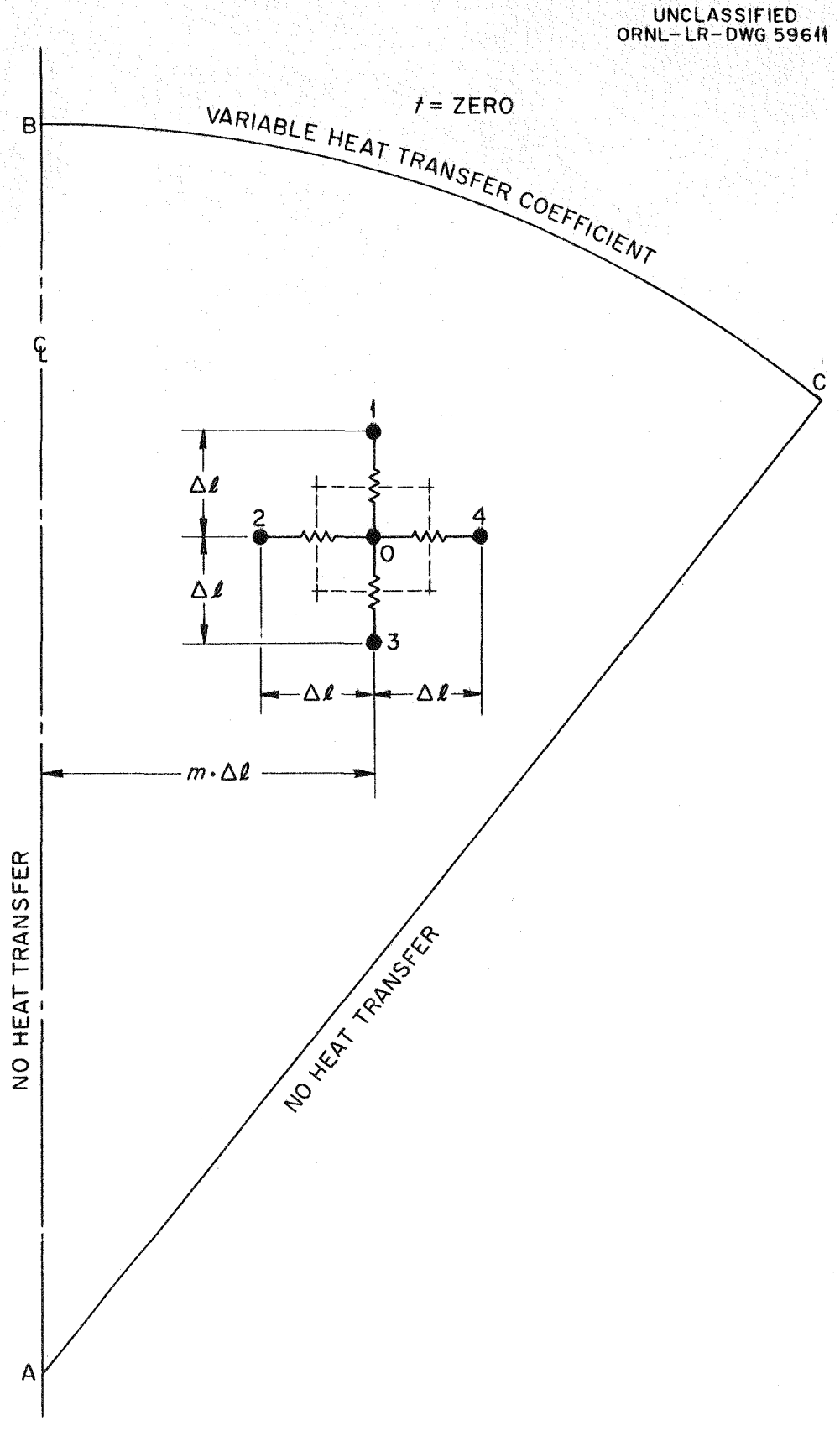
UNCLASSIFIED
ORNL-LR-DWG 59611
t = ZERO
VARIABLE HEAT TRANSFER COEFFICIENT
B
C
C
A
NO HEAT TRANSFER
NO HEAT TRANSFER
1
2
3
4
0
Δℓ
Δℓ
Δℓ
Δℓ
m·Δℓ

Fig. 11.

DISTRIBUTION

1. M. Bender
2. F. L. Carlsen
3. R. S. Carlsmith
4. R. A. Charpie
5. J. H. Coobs
6. W. B. Cottrell
7-8. F. L. Culler
9. J. Foster
10. A. P. Fraas
11. B. L. Greenstreet
12. J. D. Grimes
13. W. O. Harms
14. R. J. Hefner
15. T. Hikido
16. W. H. Jordan
17. G. W. Keilholtz
18-20. R. B. Korsmeyer
21. P. G. Lafyatis
22. H. G. MacPherson
23. W. D. Manly
24. H. C. McCurdy
25. F. H. Neill
26. M. N. Ozisik
27. A. M. Perry
28. M. W. Rosenthal
29. G. Samuels
30. H. W. Savage
31. W. L. Scott
32. O. Sisman
33. E. Storto
34. D. B. Trauger
35. A. M. Weinberg
36. M. M. Yarosh
37. ORNL-RC
38-52. Lab Records
53-67. OTIE, AEC